Dewatering methanotrophic enrichments intended for single cell protein production using biomimetic aquaporin forward osmosis membranes

Valverde Pérez, Borja; Pape, Mathias L.; Kjeldgaard, Astrid Friborg; Zachariae, August A.; Schneider, Carina; Hélix-Nielsen, Claus; Zarebska, Agata; Smets, Barth F.

Published in:
Separation and Purification Technology

Link to article, DOI:
10.1016/j.seppur.2019.116133

Publication date:
2019

Document Version
Peer reviewed version

Dewatering methanotrophic enrichments intended for single cell protein production using biomimetic aquaporin forward osmosis membranes

Borja Valverde-Pérez[a,*+], Mathias L. Pape[a+], Astrid F. Kjeldgaard[a], August A. Zachariae[a], Carina Schneider[a], Claus Hélix-Nielsen[a,b], Agata Zarebska[a], Barth F. Smets[a,*]

[a] *Department of Environmental Engineering, Technical University of Denmark, Miljøvej, Building 115, 2800 Kgs. Lyngby, Denmark*

[b] *University of Maribor, Faculty of Chemistry and Chemical Engineering, Smetanova ulica 17, 2000 Maribor, Slovenia*

**Corresponding authors: bvape@env.dtu.dk; bfsm@env.dtu.dk*

[+]*The authors have equally contributed to this work*

Keywords

Forward osmosis, biomimetic aquaporin membranes, microbial protein, water treatment, resource recovery

Abstract

Microbial biomass is becoming an alternative source of protein, especially for application in animal feeds formulations. While much progress has been made in biomass cultivation, harvesting after cultivation remains a very costly part of the overall process. This study investigated low-cost forward osmosis for dewatering methanotrophic cultures using biomimetic aquaporin membranes. Brine and glycerol were used as draw solutions as they are available as inexpensive industrial byproducts. NaCl and $MgCl_2$ were also used to better understand the behavior of brine. With NaCl and brine the highest water fluxes were obtained, but ammonium retention was low and high reverse salt fluxes were measured. With $MgCl_2$, the highest specific water flux (J_w/J_s=7.5±1.7 L g^{-1}) and a good ammonium retention (~85%) was obtained. Thus, only brines with high content on $MgCl_2$ should be considered for FO applications. With glycerol as draw solution, the solute back flux was the highest without affecting microbial growth or methane yields. Hence it shows potential as good draw solution, if available as residual stream. Surprisingly there was no significant difference in water fluxes at the different

osmotic pressures (30 and 60 atm). Noteworthy biofouling did not affect the water fluxes, except the case when NaCl at 60 atm was used as draw solution. Overall, this study demonstrates that forward osmosis is a feasible technology for harvesting methanotrophic biomass.

1. Introduction

Single-cell protein (SCP) consists of microbial biomass that can contain large amounts of nutritive proteins [1], with quality equal or better than conventional protein sources (e.g. soy or fishmeal [2]). Bacteria, yeast, and green microalgae have all been proposed as suitable protein sources for animal feed [3]. Some attempts have been made to produce SCP from synthetic or fossil fuel based resources (referred to as first generation processes). As example, methane oxidizing bacteria (MOB) are used at full scale for SCP production using natural gas and synthetic nitrogen sources [4]. However, most of the consumed proteins and nutrients, both by animals and humans, are ultimately excreted and create an environmental burden. Therefore, ongoing research focuses on the development of second generation processes for production of SCP from organic wastes or wastewaters [5–7].

Biomass harvesting or recovery is a major bottleneck in most bio-based production processes. It is resource intensive and often compromises the overall feasibility of the production process [8–10]. Membrane bioreactors (MBR) have gained interest, as they efficiently retain and up-concentrate biomass, thereby reducing costs of downstream processing (e.g., drying) [11]. Additionally, membranes can retain soluble compounds, such as organic acids or nutrients, used to grow microorganisms, and simultaneously produce purified effluents that can be reused as process or irrigation water. For this purpose micro (MF)- and ultra (UF)-filtration membranes are most commonly used [12]. These processes rely on pressure-driven filtration through porous membranes, which may lead to fouling and decreasing fluxes across the membranes [13]. Furthermore, they have limited retention capacity for soluble compounds such as ammonium [14], as the membranes pore size allows passage of nanometer size molecules. Forward osmosis (FO) has been suggested as a suitable

technology for retaining both biomass and nutrients in bioreactors [15–17]. Compared to pressure driven filtration, FO has lower energy consumption and is less prone to fouling [18]. In FO, a draw solution (DS) is used to induce a net flow of water through a semipermeable membrane into the DS from a feed solution (FS). The flow is driven by the transmembrane (difference between DS and FS) osmotic pressure gradient ($\Delta\pi$) and will occur as long as $\pi_{DS} > \pi_{FS}$. The π_{DS} arises from the DS osmolyte, which can be intentionally prepared solutions or side streams from industries (e.g., brine from desalination plants). The DS can be recovered, after use, by reverse osmosis (RO) or membrane distillation (MD), thereby producing high quality water [19,20]. Nevertheless, DS selection for FO has some challenges [21,22]: DS can be expensive, thus compromising the feasibility of the process if it is not easily recovered. Furthermore, some DS result in high solute back fluxes, which may compromise the FS quality for biotechnological applications.

The application of FO has been studied in combination with biological wastewater treatment [23], as a stand-alone water treatment technology [24] or in several biotechnological applications [11,25,26]. However, its evaluation in combination with methanotrophic biomass cultivation for microbial protein production has not yet been carried out. Therefore, this study aims to evaluate the performance of novel biomimetic aquaporin based FO membrane for dewatering active methanotrophic biomass intended for SCP production. Two low cost DS, which can be obtained as residual streams from other industrial applications have been tested. Brine is a solution with a high salt concentration produced during desalination or during other industrial processes (e.g., food industry [27]), and cannot be directly discharged into the environment [28]. To properly characterize brine as DS, its main constituent salts, $MgCl_2$ and NaCl, were also individually assessed as osmolytes. Glycerol is a byproduct from biodiesel production and a potentially cheap solute for DS preparation [29]. Two different osmotic pressures were tested to identify optimal operational conditions, using the water flux, reverse solute flux and ammonium retention as criteria. Furthermore, the impact of different DS on microbial growth and membrane biofouling were studied.

2. Materials and Methods

2.1. Flat-sheet FO membrane

The thin film composite (TFC) flat sheet FO membranes used herein are Aquaporin Inside™ membranes provided by Aquaporin A/S, Denmark. They are composed of a polyethersulfone (PES) support layer and a polyamide (PA) active layer with incorporated aquaporin proteins reconstituted in spherical polymer vesicles [30].

2.2. FO experimental setup

All FO experiments were conducted in lab-scale FO cross-flow setups with the active layer facing the feed solution side (AL-FS). Two identical FO setups were run in parallel and used for the selection of the draw solution and the evaluation of the FO performance to dewater a methanotroph active culture. A schematic representation of the setup is shown in Fig. 1. In both setups, the feed solution bottle was placed on a balance (Kern, Germany) and both feed and draw solutions were constantly mixed. The water flux J_w was determined by measuring the weight decrease of the feed solution and the reverse salt flux J_s was determined by measuring the increase in conductivity in the feed stream when using salts as draw solution. In the case of glycerol, its concentration in the FS was measured. Both weight and conductivity data were logged automatically every five minutes throughout the duration of the experiments. Samples were collected at the beginning and end of the experiment to measure pH and osmolarity.

<Figure 1>

The flat sheet membranes were mounted in a CF042A Crossflow Cell chamber (Sterlitech Corporation, USA) with two symmetric flow channels. The channels had the dimensions 85mm (length), 39mm (width) and 2.3mm (height), with an effective membrane area of 33.15cm^2. No mesh spacers were used, due to the small channel dimensions. Feed and draw solutions were recirculated in counter-current mode by a peristaltic pump (Longer

Precision Pump Co., BT100-1L, Ltd, China) achieving crossflow velocity of 4.5 cm s^{-1}. A total of 16 different experiments were run in parallel duplicates during 24 h at 20°C.

Eight different DS were prepared including NaCl, $MgCl_2$, synthetic brine and glycerol (Sigma Aldrich, USA). Synthetic representation of brine from seawater desalination was made by dissolving NaCl and $MgCl_2$ in a mass ratio of 5.4:1, which gives a Mg^{2+} to Na^+ mass ratio of 0.12 [31]. The initial volume of both FS and DS was 2 L. The concentrations of the draw solutes (Supporting information, SI-1) were chosen to yield an osmotic pressure of 30 and 60 atm by computing the van't Hoff equation.

Eight experiments were run with milli-Q water as feed solution. These experiments were used to determine the osmotic pressure that achieves highest water flux and low reverse solute fluxes. Water flux, J_w (L m^{-2} h^{-1}), was calculated as:

$$J_w = \frac{m_{FS,t2} - m_{FS,t1}}{\Delta t \cdot A \cdot \rho} \quad \text{Eq. (1)}$$

where m_{FS} is the mass of the FS (kg), A is the area of the membrane area (m^2), ρ is the water density (kg m^{-3}) and t_1 and t_2 is the start and end time of a time-step with duration Δt (h). This equation was applied to each 5 min time-step and an average flux over 24 hours was calculated as the arithmetic mean.

Similarly the reverse fluxes of draw solutes, J_s (g m^{-2} h^{-1}), were calculated from a mass balance on the feed solution as:

$$J_{s,A} = \frac{\left(V_{FS,t2} * C_{A,t2}\right) - \left(V_{FS,t1} * C_{A,t1}\right)}{A * \Delta t} \quad \text{Eq. (2)}$$

where C_A is the concentration of the solute A (g L^{-1}), V_{FS} is the volume of FS (L), A is the area of the membrane area (m^2) and t_1 and t_2 is the start and end time of a time-step with duration Δt (h). This equation was applied

to each 5 min time-step and an average flux over 24 hours was calculated as the arithmetic mean. Solute concentrations for salts were estimated from conductivity using a correlation experimentally determined for each solute (SI-1). For the case of brine, a constant Mg^{2+}/Na^{+} ratio of 0.12 was assumed. When using glycerol as DS, back flux was estimated based on the start and end volumes and glycerol concentrations. Specific water fluxes were estimated as the ratio between the water flux and the reverse solute flux (J_w/J_s) [32].

Two experiments were run with an initial ammonium concentration of 25 mg-N L^{-1} diluted in milli-Q water, using NH_4Cl as ammonium source (Sigma Aldrich, USA). These experiments were used to test the ammonium retention capacity by the membrane using brine and glycerol as draw solutions. Samples of both feed and draw solutions were taken at the beginning and end of the experiments and ammonium retention percentages were calculated in the following two ways:

$$R = \frac{C_{NH4,FS,t} * V_{FS,t}}{C_{NH4,FS,t0} * V_{FS,t0}} * 100\ \% \qquad \text{Eq. (3)}$$

$$R_{norm} = \left(1 - \frac{C_{NH4,FS,t0} * V_{FS,t0} - C_{NH4,FS,t} * V_{FS,t}}{C_{NH4,FS,t0} * \left(V_{FS,t0} - V_{FS,t}\right)}\right) * 100\ \% \qquad \text{Eq. (4)}$$

where R and and R_{Norm} are, respectively, the retention percentage and the retention percentage normalized by the trans membrane water transfer. The normalized ammonium retention is the ratio between the ammonium transferred during the experiment to the DS and the ammonium that would be transferred with the water flux in case ammonium could freely flow through the membrane. $C_{NH4,FS,t0}$ and $C_{NH4,FS,t}$ are the concentration of ammonium in the FS at the start and end of the experiment respectively (g-N L^{-1}). $\Delta C_{NH4,FS,}$ is the decrease in ammonium concentration on the FS (g-N) and ΔV is the volume of water transferred to the DS (L).

Six experiments were run using methane oxidizing bacteria cultures as feed solutions. These experiments were run to assess the impact of biofouling on FO performance. 2 days before each experiment, 1 L effluent obtained from a bubble free membrane bioreactor [33] was mixed with fresh dAMS cultivation medium to a

volume of 4.5 L in a 5 L bottle, with a septum lid. The head space was flushed with gas with a composition 60:40 of oxygen to methane at least twice per day. The bottle content was stirred with a magnetic bar (Fig.1). Thus, exponential growth phase was ensured during the test of the FO unit. When running the FO test, a gas bag with a gas composition 60:40 of oxygen to methane was connected to the top, ensuring enough gas supply for microbial growth. Liquid samples taken at the beginning and end of experiments in both FS and DS for measuring NH_3 concentration, total suspended solids (TSS) and optical density (OD) at 600 nm. For each experiment, the difference in ammonium concentration between FS at the beginning of the experiment and FS and DS at the end of the experiment was assumed to be assimilated by biomass. Gas composition on the head space was also analyzed by the end of the experiments.

Table 1 summarizes all experiments run with the FO setup.

<Table 1>

2.3. Inoculum and cultivation media

Inoculum for the different experiments was obtained from a bubble free membrane bioreactor [33], which was growing an methane oxidizing bacteria enrichment provided by Van der Ha et al. [34]. MOB were grown in dAMS, a cultivation media adapted from the dNMS media reported by Whittenbury et al. (1970), which uses ammonium chloride (Sigma Aldrich, USA) instead of nitrate as nitrogen source (SI-2). Cultivation medium was autoclaved before starting the experiments.

2.4. Biofouling characterization

Biofouling was characterized using epifluorescence microscopy. After each FO experiment, membranes were carefully stored at 4 °C for less than 24 hours prior to analysis. Staining of biomass (DNA) and polysaccharides (as surrogated of extracellular polymeric substances – EPS) was performed to characterize the biofouling. SYTO 9 (Thermo Fisher Scientific, MA, US) dissolved at 5µM in 0.9% (w/v) NaCl solution was used to target DNA,

whilst ConA (Thermo Fisher Scientific, MA, US) dissolved at 100 µg/mL in 0.1 M $NaHCO_3$ solution was used to observe α-D-mannose and α-D-glucose [36]. Pieces of membrane of about 1x1 cm size were stained in darkness for 15 min. Then, the samples were washed to remove residual staining by submerging them in 0.9% NaCl solution for 6 minutes. Washed membrane was placed in a petri dish and observed with a stereo microscope (Epifluorencence stereomicoscope, Leica MZ16 FA, Germany) at x10 magnification.

2.5. Batch assays

The protocol described by Hedegaard et al. (2018) was adapted to characterize methanotrophic activity under different concentrations of solutes used as part of DS. In brief, 250 mL serum bottles were autoclaved and closed with autoclaved Teflon caps and aluminum lids. They were filled with 85 ml of dAMS media, with the specific draw solute concentration, and inoculated with 20 ml of active biomass. After inoculation, 18.5 ml of the headspace were replaced with methane to ensure a favorable ratio of 60:40 of oxygen to methane. Batches were sampled for gas composition characterization, biomass density and ammonium concentrations. Extracted volume was replaced with a mix of atmospheric air and methane in a volumetric ratio 9:1, both filtered through 0.2 µm glass fiber filter (Sartorius, Germany). NaCl and $MgCl_2$ with concentrations 2 and 8 g L^{-1} were tested, whilst for glycerol only an initial concentration of 0.8 g L^{-1} was evaluated. These concentrations were chosen based on previous salinity inhibition studies for methanotrophs [38]. Control experiments with dAMS media were run in parallel. Experiments were run in duplicates at 20 °C.

2.6. Analytical methods

Osmolarity was measured using a freezing point osmometer (osmomat 3000, Gonotec, Germany), conductivity using a conductivity meter (Thermo Fisher Scientific, USA) and pH using a pH electrode DJ 113 (VWR, Denmark). Biomass was tracked using optical density (OD) at 600 nm (Helios™ Epsilon visible spectrophotometer, Thermo Scientific, USA) and total suspended solids (TSS) using standard APHA methods

[39]. A correlation between OD_{600} and TSS was estimated using part of the experimental data (SI-3), so TSS could be estimated as function of OD_{600} in the batch assays. Soluble compounds were measured after filtration through 0.2µm glass fiber filter (Sartorius, Germany). Ammonium, nitrite and nitrate concentrations were determined calorimetrically by a continuous-flow auto-analyzer (SKALAR San++, Netherlands). Nitrogen accumulation in biomass was estimated as the variation of total soluble nitrogen (i.e. ammonium, nitrite and nitrate) per biomass produced during the batch experiments. Glycerol concentration was measured with HPLC using an ion exclusion column (Aminex HPX-87H, Bio-Rad, USA) equipped with refractive index detector. Glycerol (cas no 56-81-5, Sigma-Aldrich, USA) was used as a reference.

Methane, carbon dioxide and oxygen content in the gas phase were monitored using gas chromatography (GC Trace 1310. Thermo Scientific), using two different columns for different gases. A HP-Plot/Q column (Agilent Technologies, USA, length 15 m, diameter 0.32 mm, film 20 µm) was used for methane and carbon dioxide, whilst HP-Molesieve column (Agilent Technologies, USA, length 30 m, diameter, 0.53, film 50 µm) was used for oxygen and methane analyses. Calibration was done by injecting gas mixtures of known concentrations (methane to carbon dioxide ratios (V V^{-1}) of 60/40, 40/30 and 5/5 for the first method; Air to methane ratios (V V^{-1}) of 100/0 and 50/50 for the second method).

3. Results and Discussion

3.1. FO performance

Experimental results from all 32 batch experiments are shown in the SI-4.

3.1.1. Milli-Q water as feed solution

Tests carried out with milli-Q water as a feed solution with the different draw solutions resulted in mean water fluxes in the range of 9.4 – 14.9 $Lm^{-2}h^{-1}$ and 8.0 – 11.1 $Lm^{-2}h^{-1}$ for initial osmotic pressure of 60 and 30 atm, respectively. As seen in Fig. 2, NaCl and brine yielded the highest water fluxes, whilst the lowest fluxes were

observed when glycerol was used as a DS solution. Similar water fluxes obtained for NaCl and brine are consistent with the high NaCl content in brine. Achilli et al. [40] found also higher water fluxes when using NaCl, compared to $MgCl_2$, as DS in a FO system using a flat-sheet cellulose triacetate membrane. Since the tested DS had similar osmotic pressure, the reduced water flux with $MgCl_2$ as DS is likely a result of the internal polarization due to lower diffusivity of divalent cations through the membrane [40–42]. In case of glycerol, much lower concentrations were required to achieve water fluxes comparable to other studies using similar aquaporin membranes [25]. For synthetic draw solutions, lower osmotic pressures are preferable, as the slightly higher water fluxes would not compensate the higher costs of a highly concentrated saline solution.

<Figure 2>

Reverse mass flux of draw solutes was lowest with $MgCl_2$ and highest with glycerol (Fig 2). Reverse solute flux with $NaCl_2$ was significantly higher than with $MgCl_2$, in agreement with previous studies [40]. Contrary to Holloway et al. [43], the addition of divalent ions (i.e., Mg^{2+}) into a DS rich in NaCl (i.e., brine in this study), did not reduce the reverse solute flux. Specific water fluxes (Table 2) indicate that $MgCl_2$ had the best performance with an average of 7.5 ± 1.7 L g^{-1} compared to 1.8 ± 0.2 L g^{-1} for glycerol, 4.0 ± 0.4 L g^{-1} for brine and 4.2 ± 1.1 L g^{-1} for NaCl respectively. However, when comparing molar reverse solute fluxes (SI-4), glycerol ranks better, as the back flux values are comparable to those with NaCl and brine as DS. Nevertheless, it is still clear that $MgCl_2$ is the least prone solute to migrate through the membrane to the FS. For all cases except $MgCl_2$, a higher osmotic pressure leads to higher reverse solute flux. For all cases J_w/J_s ratios are comparably higher compared to other studies [40], where J_w/J_s ratios were 1.72 L g^{-1} for $MgCl_2$ and 1.33 L g^{-1} for NaCl.

<Table 2>

3.1.2.Ammonium solution as feed solution

The ammonium retention experiment using brine as DS resulted in average water fluxes of 11.4±0.4 L m^{-2} h^{-1}, similar to the water flux observed in the milli-Q water experiment using 30 atm brine as DS (Fig. 1). Testing

ammonium retention with glycerol yielded an average water flux of 8.6 ±0.2 L m^{-2} h^{-1}, slightly higher than the water flux from the milli-Q water experiment (Fig. 1). The reverse solute flux was unchanged when using glycerol as DS, whilst for brine was not reported (measured conductivity was dependent on both ammonium and solute fluxes across the membrane and thus relations presented in SI-1 could not be applied). The retention percentages for both experiments are shown in Fig.3. For glycerol an average ammonium retention of 93.4 ±2.2% (normalized: 81±6%) was observed, which is within the range reported by other studies [15,19]. However, a low retention of 51±4.7% (normalized: -7±8%) was observed with brine. The low normalized retention for brine indicates that ammonium crosses the membrane faster than water (i.e., active transport). Active transport can be a consequence of cation exchange through the membrane, whereby for every Na^+ cation transferred to the FS an NH_4^+ cation is transferred to the DS [44]. Indeed, recent studies have obtained positive correlations between Na^+ back flux and NH_4^+ forward flux when using biomimetic membranes at pH lower than 9 in the DS [45], which is higher than the pH used in our experiments (Table S4). Therefore, the authors concluded that DS using solutes without charge (e.g., glycerol) work best for ammonium retention when using biomimetic membranes for forward osmosis.

<Figure 3>

3.1.3.Active methanotrophic culture as feed solution

With methanotrophic culture suspension as FS mean water fluxes remained similar to those using milli-Q water as FS. High concentration factor (CF=1.5-2; SI-4) were achieved. Concentration factor is a critical parameter for assessing dewaterability of biomass by traditional pressure driven membrane processes like reverse osmosis, where internal concentration polarization limits the water extraction and thus the biomass recovery. Furthermore, lack of significant flux decline indicates low influence of fouling on membrane performance (Fig.4). This is in agreement with findings reported in literature [13,46–48]. Therefore, FO seems to be a suitable process for methanotrophic biomass dewatering. Other applications show very sharp decrease on

water fluxes after 24 hours [49,50]. The comparably lower fouling propensity can be explained by the fact that most existing applications for water treatment deal with complex FS with rather complex matrices [15]. However, for safe production of high quality microbial protein, it is important to produce relatively clean cultivation media based on used resources (e.g., nutrients may be extracted from residual streams before fed to the microbes [51]). Therefore, the tested conditions are similar to those of a full scale implementation of this process.

<Figure 4>

Ammonium retention in these experiments was similar to the observations made with ammonium solutions as FS. Glycerol led to the highest retention (all ammonium was assimilated or kept in the FS), whilst NaCl and brine yielded the lowest rejection (Fig.5). When using $MgCl_2$ as DS, ammonium retention was significantly higher than the retention obtained with NaCl as DS. Furthermore, results were comparable to earlier reported ammonium retentions for the same Aquaporin membranes using also $MgCl_2$ as DS, which ranged between 80 and 99 % [14]. Fig. 5 shows the fate of ammonium by the end of the test. When analysing normalized ammonium retention, NaCl or brine as DS resulted in the lowest retention. Furthermore, when using NaCl at 30 atm as DS, ammonium is actively transferred through the membrane yielding to a normalized retention of -17.9±3.7%. $MgCl_2$ DS yielded considerable better retentions and always positive normalized retentions (SI-4), suggesting that ammonium is mostly exchanged by Na^+ when using brine as DS. A possible explanation for the higher ammonium retention with $MgCl_2$ as a DS can be found when considering the Donnan equilibrium [52]. Due to its smaller atom size, the reverse diffusion of Cl^- ions usually exceeds that of Mg_2^+ ions. This leads to a charge imbalance that prompts anions diffusion from the FS to the DS in order to restore the charge equilibrium while leading to an accumulation of cationic ammonium in the FS.

<Figure 5>

All experiments showed similar biofouling trends, regardless the DS. After 24 hours, cells mostly accumulated on the membranes (Fig. 6 a) with minor amount of polysaccharides (Fig. 6 b), indicating initial colonization of membrane by bacteria. Therefore, most of the fouling after 24h is due to physical conditions (e.g., pressure of the water going through the membrane) rather than biological activity (i.e., biofilm formation). Biomass was loosely bounded as it was easily detached with physical cleaning (e.g., surface washing with deionized water). Longer term operation may allow the formation of biofilms [49], which would require more costly cleaning methods [53].

<Figure 6>

3.2 Impact of draw solutes on methanotrophic activity and FO performance

Similar specific growth rates, around 1 d^{-1}, were measured in control and experiments with glycerol and low concentrations of $MgCl_2$ and NaCl levels (Table 3). This is in agreement with growth rates reported in literature for methanotrophic biomass [54,55]. High salt concentrations inhibited methanotrophic growth. Growth rates were reduced by 57 % and 94 % when growing methanotrophs at 8 g L^{-1} NaCl and $MgCl_2$, respectively. The decrease in methane oxidation activity has previously been reported for NaCl [38,56]. However, our study shows that MOB are more sensitive to $MgCl_2$, demonstrating that the impact of salinity depends on the ions in solution. Growth yield of methane for the control is 0.57±0.03 g-VSS g^{-1}-CH_4, which falls within the data reported in previous studies [57–61]. As salt concentration increases, the methane yield decreases. High salinity commonly leads to higher energy demand for cellular maintenance [62,63], which explains the higher methane consumption per methanotrophic biomass produced. In case of glycerol, yields are slightly higher. Glycerol concentrations decrease during the experiment (SI-5), probably due to consumption by heterotrophic bacteria growing in the consortium. Most methane oxidizing bacteria are strict methanotrophs and cannot consume other carbon sources, such as glycerol [64]. Products from ammonia oxidation, i.e. nitrite and nitrate,

were not found in any of the batch experiments. Thus, the main nitrogen removal process is assumed to be microbial assimilation. Highest nitrogen assimilation was found for the control and the experiment with NaCl at 8 g L^{-1}. Nevertheless, nitrogen assimilation by biomass was comparable for all experiments (Table 3), suggesting that salt concentration may have a limited effect on protein storage. Nitrogen assimilation rates were comparably higher than reported in other studies [59,65]. During the experiments, the salt had an impact on flocculation (SI-5), with increased flocculation at higher salinity levels. This could be a consequence of the production of extracellular polymers due to the salt stress [66] as well as the impact on cell surface charge [67]. Overall, results suggest using glycerol as DS because of the limited impact of the back fluxes on methanotrophs growth and ammonia assimilation.

<Table 3>

4. Conclusion

FO process was investigated as a method for methanotrophic culture dewatering, thus potentially reducing the downstream costs for microbial protein production. Different DS solutions were evaluated at different osmotic pressures in order to find the most cost-efficient operational conditions. $MgCl_2$ showed the highest J_w/J_s, with similar performance for both 30 and 60 atm as osmotic pressure. However, ammonium retention from the feed solution was compromised as 14-16% of the fed ammonium was transferred to the DS. NaCl and brine gave highest J_w, but also large solute back fluxes. Strikingly, the use of NaCl resulted in active ammonia transfer from the FS to the DS, thus showing worst ammonia retention performance (44-53% of ammonium leaked through the FO membrane). NaCl partially inhibited methanotrophic growth at high concentrations (53% reduction at 8 g L^{-1}), whilst $MgCl_2$ prevented any biomass growth when concentration was 8 g L^{-1}. Thus, it was concluded that brine, despite being cheap DS, should not be employed in applications where the FS is rich on ammonium. Glycerol showed the highest ammonium retention and, despite the high back flux to the FS, no impact on microbial growth was demonstrated. Thus, our results suggest glycerol performs best among all tested DS.

Acknowledgment

We would like to thank Dr. Arnaud Dechesne for his assistance on the image analysis to characterize membrane biofouling. We would like to thank Aquaporin A/S for providing the FO membranes. This work was partly supported by the Innovation Fund Denmark (Project MEMENTO grant No. 4106-00021B) and Novo Nordisk Foundation (Project BioCAT Grant No. NNF14OC0011277).

References

[1] Anupama, P. Ravindra, Value-added food:: Single cell protein, Biotechnol. Adv. 18 (2000) 459–479. doi:10.1016/S0734-9750(00)00045-8.

[2] M. Øverland, A.-H. Tauson, K. Shearer, A. Skrede, Evaluation of methane-utilising bacteria products as feed ingredients for monogastric animals, Arch. Anim. Nutr. 64 (2010) 171–189. doi:10.1080/17450391003691534.

[3] M. D'Este, M. Alvarado-Morales, I. Angelidaki, Amino acids production focusing on fermentation technologies – A review, Biotechnol. Adv. (2017). doi:10.1016/j.biotechadv.2017.09.001.

[4] E. B. Larsen, U-shape and/or nozzle-u-loop fermentor and method of carrying out a fermentation process, 2000.

[5] Z. Rasouli, B. Valverde-Pérez, M. D'Este, D. De Francisci, I. Angelidaki, Nutrient recovery from industrial wastewater as single cell protein by a co-culture of green microalgae and methanotrophs, Biochem. Eng. J. 134 (2018) 129–135. doi:10.1016/J.BEJ.2018.03.010.

[6] T. Hülsen, K. Hsieh, Y. Lu, S. Tait, D.J. Batstone, Simultaneous treatment and single cell protein production from agri-industrial wastewaters using purple phototrophic bacteria or microalgae – A comparison, Bioresour. Technol. 254 (2018) 214–223. doi:10.1016/J.BIORTECH.2018.01.032.

[7] B. Khoshnevisan, P. Tsapekos, Y. Zhang, B. Valverde-Pérez, I. Angelidaki, Urban biowaste valorization by coupling anaerobic digestion and single cell protein production, Bioresour. Technol. 290 (2019) 121743. doi:10.1016/J.BIORTECH.2019.121743.

[8] P. Pal, J. Sikder, S. Roy, L. Giorno, Process intensification in lactic acid production: A review of membrane based processes, Chem. Eng. Process. Process Intensif. 48 (2009) 1549–1559. doi:10.1016/J.CEP.2009.09.003.

[9] D.S. Wágner, M. Radovici, B.F. Smets, I. Angelidaki, B. Valverde-Pérez, B.G. Plósz, Harvesting microalgae using activated sludge can decrease polymer dosing and enhance methane production via co-digestion in a bacterial-microalgal process, Algal Res. 20 (2016). doi:10.1016/j.algal.2016.10.010.

[10] N. Pragya, K.K. Pandey, P.K. Sahoo, A review on harvesting, oil extraction and biofuels production technologies from microalgae, Renew. Sustain. Energy Rev. 24 (2013) 159–171.

doi:10.1016/J.RSER.2013.03.034.

[11] T. Mazzuca Sobczuk, M.J. Ibáñez González, E. Molina Grima, Y. Chisti, Forward osmosis with waste glycerol for concentrating microalgae slurries, Algal Res. 8 (2015) 168–173. doi:10.1016/J.ALGAL.2015.02.008.

[12] C. Charcosset, Membrane processes in biotechnology: An overview, Biotechnol. Adv. 24 (2006) 482–492. doi:10.1016/J.BIOTECHADV.2006.03.002.

[13] X. Wang, V.W.C. Chang, C.Y. Tang, Osmotic membrane bioreactor (OMBR) technology for wastewater treatment and reclamation: Advances, challenges, and prospects for the future, J. Memb. Sci. 504 (2016) 113–132. doi:10.1016/J.MEMSCI.2016.01.010.

[14] A. Zarebska, D. Romero Nieto, K. V. Christensen, L. Fjerbæk Søtoft, B. Norddahl, Ammonium Fertilizers Production from Manure: A Critical Review, Crit. Rev. Environ. Sci. Technol. 45 (2015) 1469–1521. doi:10.1080/10643389.2014.955630.

[15] C. Schneider, R.S. Rajmohan, A. Zarebska, P. Tsapekos, C. Hélix-Nielsen, Treating anaerobic effluents using forward osmosis for combined water purification and biogas production, Sci. Total Environ. 647 (2019) 1021–1030. doi:10.1016/J.SCITOTENV.2018.08.036.

[16] T. Yan, Y. Ye, H. Ma, Y. Zhang, W. Guo, B. Du, Q. Wei, D. Wei, H.H. Ngo, A critical review on membrane hybrid system for nutrient recovery from wastewater, Chem. Eng. J. 348 (2018) 143–156. doi:10.1016/J.CEJ.2018.04.166.

[17] A.J. Ansari, F.I. Hai, W.E. Price, J.E. Drewes, L.D. Nghiem, Forward osmosis as a platform for resource recovery from municipal wastewater - A critical assessment of the literature, J. Memb. Sci. 529 (2017) 195–206. doi:10.1016/J.MEMSCI.2017.01.054.

[18] Q. Ge, M. Ling, T.-S. Chung, Draw solutions for forward osmosis processes: Developments, challenges, and prospects for the future, J. Memb. Sci. 442 (2013) 225–237. doi:10.1016/J.MEMSCI.2013.03.046.

[19] R.W. Holloway, A.E. Childress, K.E. Dennett, T.Y. Cath, Forward osmosis for concentration of anaerobic digester centrate, Water Res. 41 (2007) 4005–4014. doi:10.1016/J.WATRES.2007.05.054.

[20] Q. Liu, C. Liu, L. Zhao, W. Ma, H. Liu, J. Ma, Integrated forward osmosis-membrane distillation process for human urine treatment, Water Res. 91 (2016) 45–54. doi:10.1016/J.WATRES.2015.12.045.

[21] D.L. Shaffer, J.R. Werber, H. Jaramillo, S. Lin, M. Elimelech, Forward osmosis: Where are we now?, Desalination. 356 (2015) 271–284. doi:10.1016/J.DESAL.2014.10.031.

[22] S. Roy, S. Ragunath, S. Roy, S. Ragunath, Emerging Membrane Technologies for Water and Energy Sustainability: Future Prospects, Constrains and Challenges, Energies. 11 (2018) 2997. doi:10.3390/en11112997.

[23] J. Korenak, S. Basu, M. Balakrishnan, C. Hélix-Nielsen, I. Petrinic, Forward Osmosis in Wastewater Treatment Processes, Acta Chim. Slov. 64 (2017) 83–94. doi:10.17344/acsi.2016.2852.

[24] T. Hey, N. Bajraktari, Å. Davidsson, J. Vogel, H.T. Madsen, C. Hélix-Nielsen, J. la C. Jansen, K. Jönsson,

Evaluation of direct membrane filtration and direct forward osmosis as concepts for compact and energy-positive municipal wastewater treatment, Environ. Technol. 39 (2018) 264–276. doi:10.1080/09593330.2017.1298677.

[25] S. Kalafatakis, S. Braekevelt, A. Lymperatou, A. Zarebska, C. Hélix-Nielsen, L. Lange, I. V. Skiadas, H.N. Gavala, Application of forward osmosis technology in crude glycerol fermentation biorefinery-potential and challenges, Bioprocess Biosyst. Eng. 41 (2018) 1089–1101. doi:10.1007/s00449-018-1938-8.

[26] F.M. Munshi, J. Church, R. McLean, N. Maier, A.H.M.A. Sadmani, S.J. Duranceau, W.H. Lee, Dewatering algae using an aquaporin-based polyethersulfone forward osmosis membrane, Sep. Purif. Technol. 204 (2018) 154–161. doi:10.1016/J.SEPPUR.2018.04.077.

[27] N. Fucà, D.J. McMahon, M. Caccamo, L. Tuminello, S. La Terra, M. Manenti, G. Licitra, Effect of brine composition and brining temperature on cheese physical properties in Ragusano cheese, J. Dairy Sci. 95 (2012) 460–470. doi:10.3168/JDS.2011-4438.

[28] B.K. Pramanik, L. Shu, V. Jegatheesan, A review of the management and treatment of brine solutions, Environ. Sci. Water Res. Technol. 3 (2017) 625–658. doi:10.1039/C6EW00339G.

[29] Z. Gholami, A.Z. Abdullah, K.-T. Lee, Dealing with the surplus of glycerol production from biodiesel industry through catalytic upgrading to polyglycerols and other value-added products, Renew. Sustain. Energy Rev. 39 (2014) 327–341. doi:10.1016/J.RSER.2014.07.092.

[30] Y. Zhao, C. Qiu, X. Li, A. Vararattanavech, W. Shen, J. Torres, C. Hélix-Nielsen, R. Wang, X. Hu, A.G. Fane, C.Y. Tang, Synthesis of robust and high-performance aquaporin-based biomimetic membranes by interfacial polymerization-membrane preparation and RO performance characterization, J. Memb. Sci. 423–424 (2012) 422–428. doi:10.1016/J.MEMSCI.2012.08.039.

[31] S. Tepavitcharova, T. Todorov, D. Rabadjieva, M. Dassenakis, V. Paraskevopoulou, Chemical speciation in natural and brine sea waters, Environ. Monit. Assess. 180 (2011) 217–227. doi:10.1007/s10661-010-1783-y.

[32] D. Qin, Z. Liu, Z. Liu, H. Bai, D.D. Sun, Superior Antifouling Capability of Hydrogel Forward Osmosis Membrane for Treating Wastewaters with High Concentration of Organic Foulants, Environ. Sci. Technol. 52 (2018) 1421–1428. doi:10.1021/acs.est.7b04838.

[33] B. Valverde-Pérez, B., Xing, W., Zachariae, A. Z., Kjeldgaard, A. F., Skadborg, M. M., Palomo, A., and B.F. Smets, Microbial protein production using a novel bubble-free membrane bioreactor, IWA Nutr. Remov. Recover. Conf., Brisbane, (2018).

[34] D. van der Ha, B. Bundervoet, W. Verstraete, N. Boon, A sustainable, carbon neutral methane oxidation by a partnership of methane oxidizing communities and microalgae, Water Res. 45 (2011) 2845–2854. doi:10.1016/j.watres.2011.03.005.

[35] R. Whittenbury, J.F. Wilkinson, Enrichment, Isolation and Some Properties of Me thane-utilizing Bacteria, J. Gen. Microbiol. 61 (1970) 205–218.

[36] C. Pellicer-Nàcher, B.F. Smets, Structure, composition, and strength of nitrifying membrane-aerated biofilms, Water Res. 57 (2014) 151–161. doi:10.1016/J.WATRES.2014.03.026.

[37] M.J. Hedegaard, H. Deliniere, C. Prasse, A. Dechesne, B.F. Smets, H.-J. Albrechtsen, Evidence of co-metabolic bentazone transformation by methanotrophic enrichment from a groundwater-fed rapid sand filter, Water Res. 129 (2018) 105–114. doi:10.1016/J.WATRES.2017.10.073.

[38] D. Van Der Ha, S. Hoefman, P. Boeckx, W. Verstraete, N. Boon, Copper enhances the activity and salt resistance of mixed methane-oxidizing communities, (2010). doi:10.1007/s00253-010-2702-4.

[39] APHA, American Water Works Association, Water Environment Federation, Standard methods for the examination of water and wastewater, Washington DC, 1999.

[40] A. Achilli, T.Y. Cath, A.E. Childress, Selection of inorganic-based draw solutions for forward osmosis applications, J. Memb. Sci. 364 (2010) 233–241. doi:10.1016/J.MEMSCI.2010.08.010.

[41] N.T. Hancock, T.Y. Cath, Solute Coupled Diffusion in Osmotically Driven Membrane Processes, Environ. Sci. Technol. 43 (2009) 6769–6775. doi:10.1021/es901132x.

[42] K.S. Bowden, A. Achilli, A.E. Childress, Organic ionic salt draw solutions for osmotic membrane bioreactors, Bioresour. Technol. 122 (2012) 207–216. doi:10.1016/J.BIORTECH.2012.06.026.

[43] R.W. Holloway, R. Maltos, J. Vanneste, T.Y. Cath, Mixed draw solutions for improved forward osmosis performance, J. Memb. Sci. 491 (2015) 121–131. doi:10.1016/J.MEMSCI.2015.05.016.

[44] X. Lu, C. Boo, J. Ma, M. Elimelech, Bidirectional Diffusion of Ammonium and Sodium Cations in Forward Osmosis: Role of Membrane Active Layer Surface Chemistry and Charge, Environ. Sci. Technol. 48 (2014) 14369–14376. doi:10.1021/es504162v.

[45] K.C. Kedwell, M.L. Christensen, C.A. Quist-Jensen, M.K. Jørgensen, Effect of reverse sodium flux and pH on ammoniacal nitrogen transport through biomimetic membranes, Sep. Purif. Technol. 217 (2019) 40–47. doi:10.1016/J.SEPPUR.2019.02.001.

[46] E.A. Bell, R.W. Holloway, T.Y. Cath, Evaluation of forward osmosis membrane performance and fouling during long-term osmotic membrane bioreactor study, J. Memb. Sci. 517 (2016) 1–13. doi:10.1016/J.MEMSCI.2016.06.014.

[47] B. Corzo, T. de la Torre, C. Sans, R. Escorihuela, S. Navea, J.J. Malfeito, Long-term evaluation of a forward osmosis-nanofiltration demonstration plant for wastewater reuse in agriculture, Chem. Eng. J. 338 (2018) 383–391. doi:10.1016/J.CEJ.2018.01.042.

[48] J. Korenak, C. Hélix-Nielsen, H. Bukšek, I. Petrinić, Efficiency and economic feasibility of forward osmosis in textile wastewater treatment, J. Clean. Prod. 210 (2019) 1483–1495. doi:10.1016/J.JCLEPRO.2018.11.130.

[49] B. Yuan, X. Wang, C. Tang, X. Li, G. Yu, In situ observation of the growth of biofouling layer in osmotic membrane bioreactors by multiple fluorescence labeling and confocal laser scanning microscopy, Water Res. 75 (2015) 188–200. doi:10.1016/J.WATRES.2015.02.048.

[50] N.C. Nguyen, S.-S. Chen, H.-Y. Yang, N.T. Hau, Application of forward osmosis on dewatering of high nutrient sludge, Bioresour. Technol. 132 (2013) 224–229. doi:10.1016/J.BIORTECH.2013.01.028.

[51] M.E.R. Christiaens, S. Gildemyn, S. Matassa, T. Ysebaert, J. De Vrieze, K. Rabaey, Electrochemical Ammonia Recovery from Source-Separated Urine for Microbial Protein Production, Environ. Sci. Technol. 51 (2017) 13143–13150. doi:10.1021/acs.est.7b02819.

[52] T. Hu, X. Wang, C. Wang, X. Li, Y. Ren, Impacts of inorganic draw solutes on the performance of thin-film composite forward osmosis membrane in a microfiltration assisted anaerobic osmotic membrane bioreactor, RSC Adv. 7 (2017) 16057–16063. doi:10.1039/C7RA01524K.

[53] Y. Chun, D. Mulcahy, L. Zou, I.S. Kim, A Short Review of Membrane Fouling in Forward Osmosis Processes., Membranes (Basel). 7 (2017). doi:10.3390/membranes7020030.

[54] J.-P. Arcangeli, E. Arvin, Modelling the growth of a methanotrophic biofilm: Estimation of parameters and variability, Biodegradation. 10 (1999) 177–191. doi:10.1023/A:1008317906069.

[55] J. Lee, N. Jang, M. Yasin, E.Y. Lee, I.S. Chang, C. Kim, Enhanced mass transfer rate of methane via hollow fiber membrane modules for Methylosinus trichosporium OB3b fermentation, J. Ind. Eng. Chem. 39 (2016) 149–152. doi:10.1016/j.jiec.2016.05.019.

[56] S. Schnell, G.M. King, Responses of methanotrophic activity in soils and cultures to water stress., Appl. Environ. Microbiol. 62 (1996) 3203–9.

[57] A. AlSayed, A. Fergala, S. Khattab, A. Eldyasti, Kinetics of type I methanotrophs mixed culture enriched from waste activated sludge, Biochem. Eng. J. 132 (2018) 60–67. doi:10.1016/J.BEJ.2018.01.003.

[58] J.H. Harwood, S.J. Pirt, Quantitative Aspects of Growth of the Methane Oxidizing Bacterium *Methylococcus capsulatus* on Methane in Shake Flask and Continuous Chemostat Culture, J. Appl. Bacteriol. 35 (1972) 597–607. doi:10.1111/j.1365-2672.1972.tb03741.x.

[59] A.G. Zhivotchenko, E.S. Nikonova, M.H. Jørgensen, Copper effect on the growth kinetics of Methylococcus capsulatus (bath), Biotechnol. Tech. 9 (1995) 163–168. doi:10.1007/BF00157072.

[60] D.J. Leak, H. Dalton, Growth yields of methanotrophs, Appl. Microbiol. Biotechnol. 23 (1986) 470–476. doi:10.1007/BF02346062.

[61] K.H. Rostkowski, A.R. Pfluger, C.S. Criddle, Stoichiometry and kinetics of the PHB-producing Type II methanotrophs Methylosinus trichosporium OB3b and Methylocystis parvus OBBP, Bioresour. Technol. 132 (2013) 71–77. doi:10.1016/J.BIORTECH.2012.12.129.

[62] R. Olz, K. Larsson, L. Adler, L. Gustafsson, Energy flux and osmoregulation of Saccharomyces cerevisiae grown in chemostats under NaCl stress., J. Bacteriol. 175 (1993) 2205–13. doi:10.1128/JB.175.8.2205-2213.1993.

[63] L. Welles, C.M. Lopez-Vazquez, C.M. Hooijmans, M.C.M. van Loosdrecht, D. Brdjanovic, Impact of salinity on the anaerobic metabolism of phosphate-accumulating organisms (PAO) and glycogen-accumulating organisms (GAO), Appl. Microbiol. Biotechnol. 98 (2014) 7609–7622. doi:10.1007/s00253-014-5778-4.

[64] J.D. Semrau, A.A. DiSpirito, S. Vuilleumier, Facultative methanotrophy: false leads, true results, and suggestions for future research, FEMS Microbiol. Lett. 323 (2011) 1–12. doi:10.1111/j.1574-

6968.2011.02315.x.

[65] M. Veillette, P. Viens, A.A. Ramirez, R. Brzezinski, M. Heitz, Effect of ammonium concentration on microbial population and performance of a biofilter treating air polluted with methane, Chem. Eng. J. 171 (2011) 1114–1123. doi:10.1016/J.CEJ.2011.05.008.

[66] E. Reid, X. Liu, S.J. Judd, Effect of high salinity on activated sludge characteristics and membrane permeability in an immersed membrane bioreactor, J. Memb. Sci. 283 (2006) 164–171. doi:10.1016/J.MEMSCI.2006.06.021.

[67] A. Zita, M. Hermansson, Effects of ionic strength on bacterial adhesion and stability of flocs in a wastewater activated sludge system., Appl. Environ. Microbiol. 60 (1994) 3041–8.

Figures

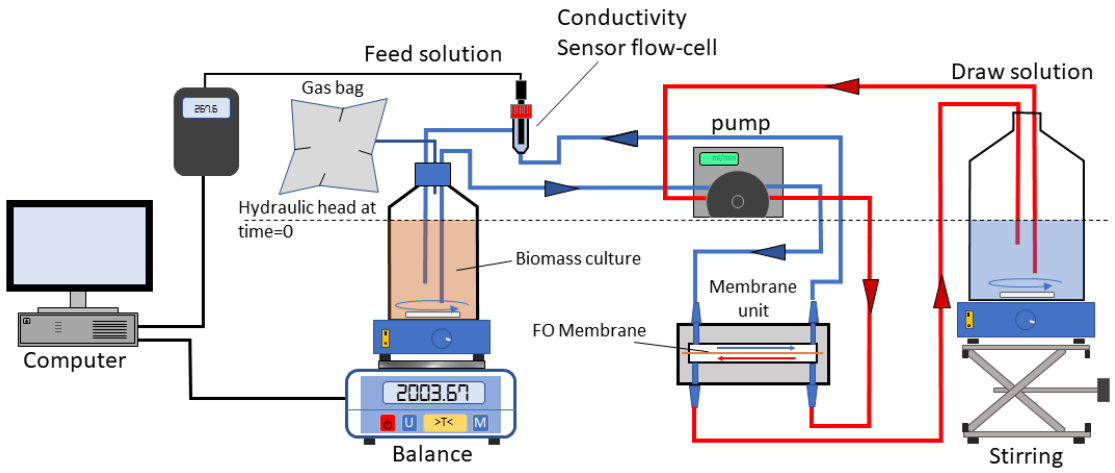

Figure 1 Setup for FO experiments. The scheme represents the experiments run using active methanotrophs in the feed solution. For experiments run with milli-Q water or milli-Q water with ammonium the setup was the same, but without the gas bag connected in the 5 L feed solution bottle.

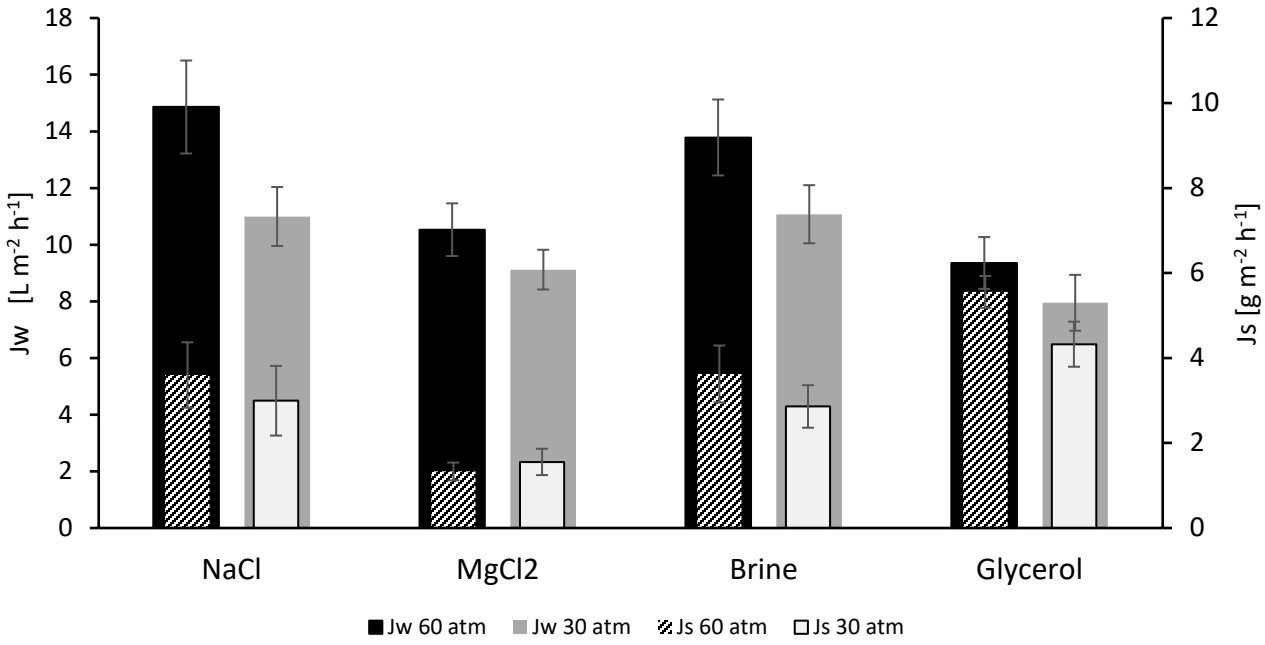

Figure 2 Water (J_w) and reverse solute (J_s) fluxes in FO experiments with milli-Q water as feed solution and four different draw solutes with initial osmotic pressure of 60 bar (black) and 30 bar (grey) respectively. Error bars represent standard deviation of the duplicate results.

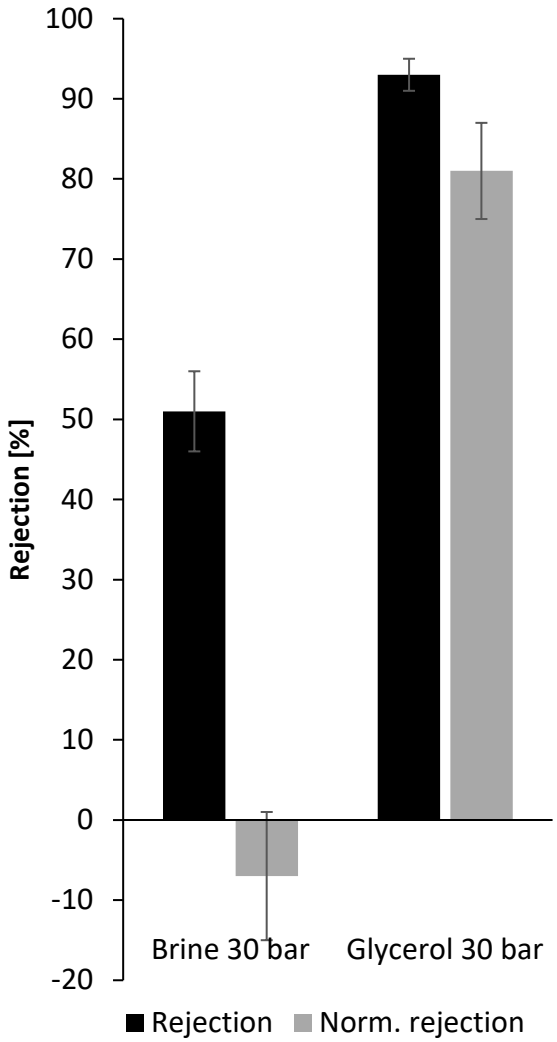

Figure 3 Rejection percentages, for the ammonium rejection experiments with brine and glycerol.

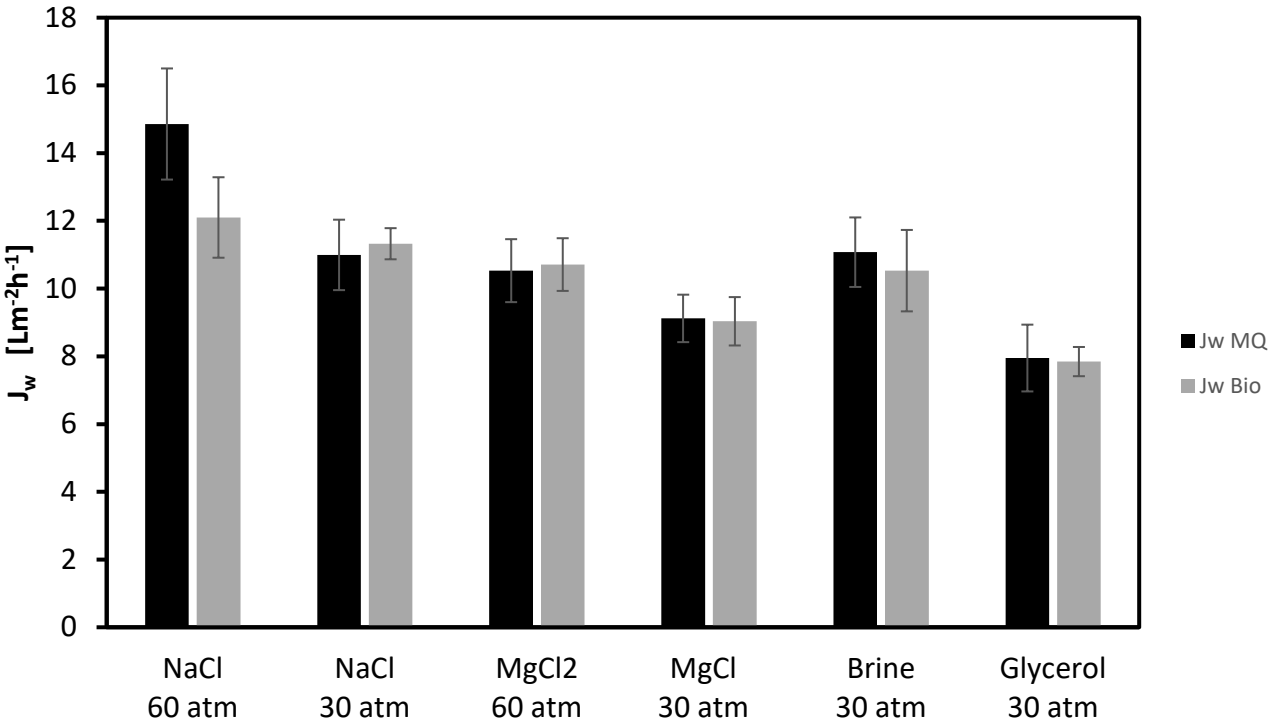

Figure 2 Water flux from the biofouling (grey) and milli-Q water experiments (black).

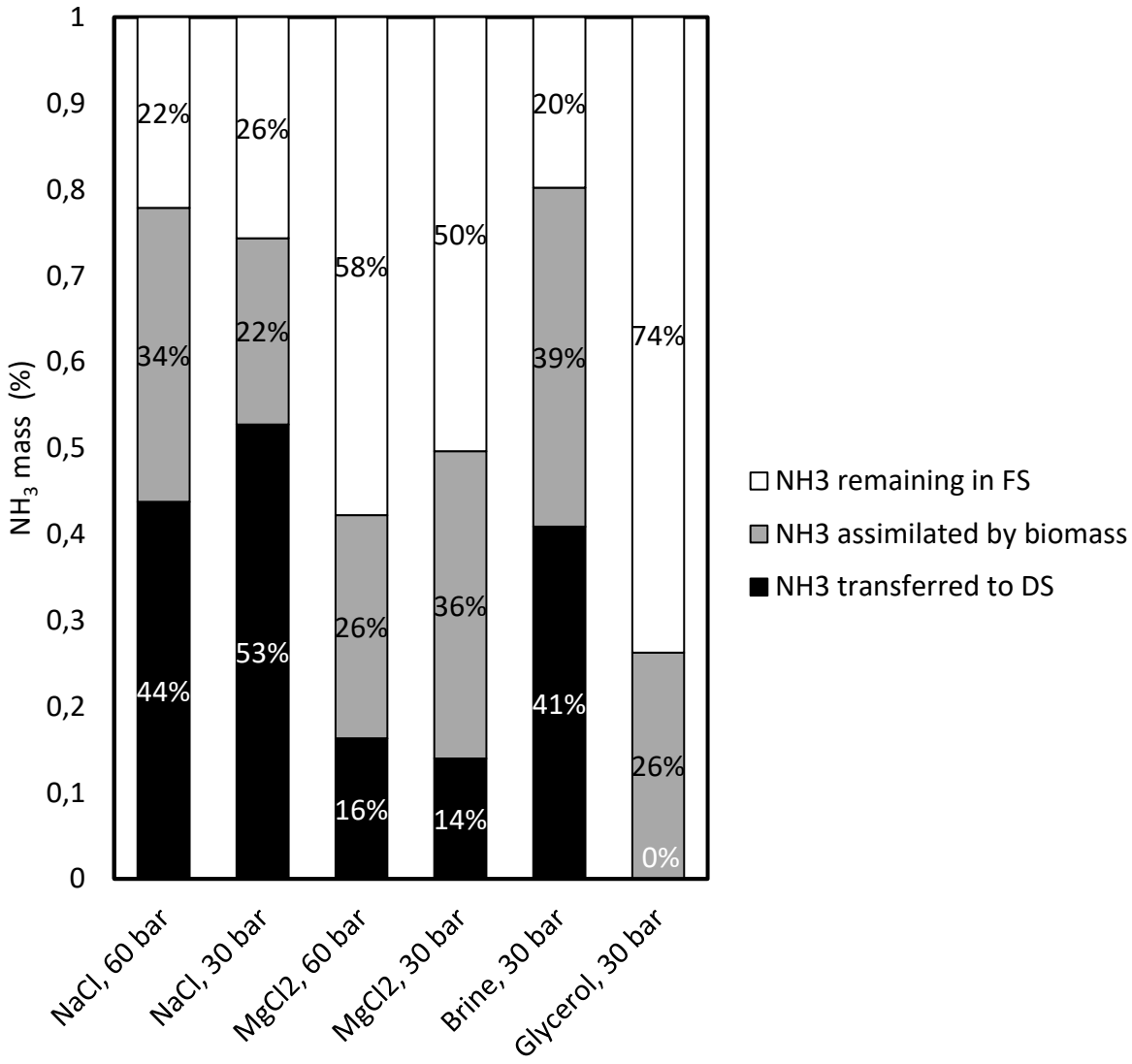

Figure 3 Fate of ammonium during the experiments using active methanotrophic biomass as FS.

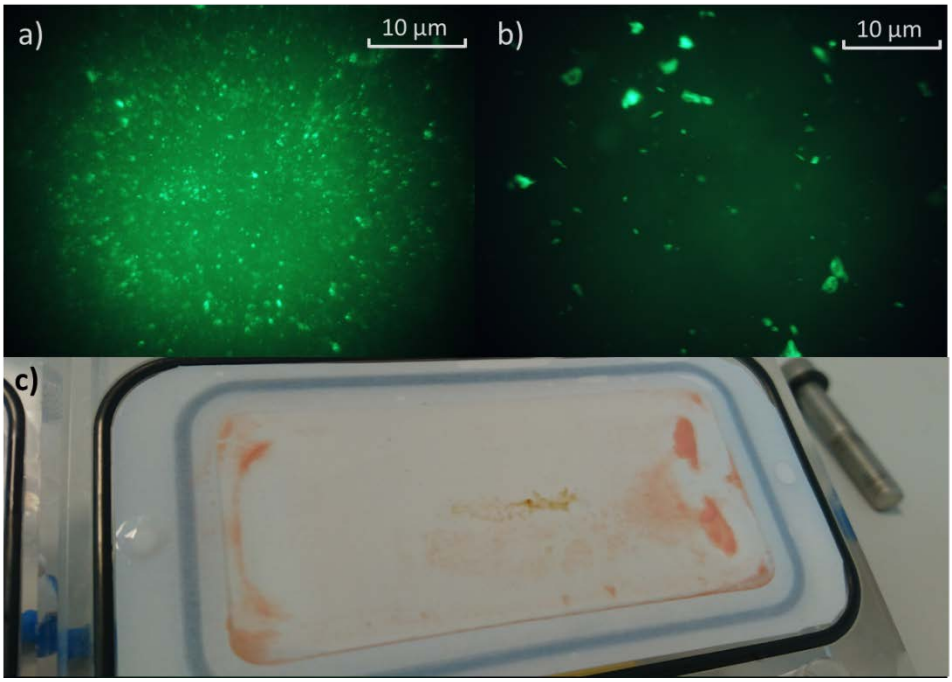

Figure 6 Membranes at the end of the experiments using active methanotrophic cultures as FS and brine as DS: a) stained cells; b) stained polysaccharides; c) membrane at the end of the experiment.

Tables

Table 1 Summary of FO experiments

	Feed Solution (FS)	Draw solution (DS)	DS osmotic pressure (atm)	Experiment goal
1	MQ-water	NaCl	60	Effect of osmotic pressure in DS on J_w and J_s
2	MQ-water	NaCl	30	
3	MQ-water	$MgCl_2$	60	
4	MQ-water	$MgCl_2$	30	
5	MQ-water	Brine	60	
6	MQ-water	Brine	30	
7	MQ-water	Glycerol	60	
8	MQ-water	Glycerol	30	
9	MQ-water (25 mg L^{-1} NH_3)	Brine	30	Ammonia retention
10	MQ-water (25 mg L^{-1} NH_3)	Glycerol	30	
11	MOB in dAMS	$MgCl_2$	30	Impact of biofouling on J_w and J_s
12	MOB in dAMS	$MgCl_2$	60	
13	MOB in dAMS	NaCl	30	
14	MOB in dAMS	NaCl	60	
15	MOB in dAMS	Glycerol	30	
16	MOB in dAMS	Brine	30	

Table 2 Ratio of water flux to reverse salt flux [L g^{-1}].

	Draw solution (DS)	DS osmotic pressure (atm)	J_w/J_s (L g^{-1})
1	NaCl	60	4.24±1.02
2	NaCl	30	3.89±1.13
3	$MgCl_2$	60	8±1.45
4	$MgCl_2$	30	6.02±1.28
5	Brine	60	3.83±0.8
6	Brine	30	3.9±0.77
7	Glycerol	60	1.69±0.2
8	Glycerol	30	1.86±0.32

Table 3 Growth rates and methane yields for methanotrophic enrichment at different solute concentrations

	Control	Glycerol	NaCl		$MgCl_2$	
		0.8 g L^{-1}	2 g L^{-1}	8 g L^{-1}	2 g L^{-1}	8 g L^{-1}
Growth rate (d^{-1})	0.91±0.19	0.82±0.08	0.8±0.09	0.48±0.12	1.02±0.17	0.08±0.11
Yield g-VSS g^{-1}-CH_4	0.57±0.03	0.65±0.05	0.48±0.01	0.5±0.08	0.43±0.03	0.09±0.09
Nitrogen content in biomass g-N g^{-1}-VSS	0.27±0.08	0.21±0.03	0.21±0.06	0.29±0.14	0.2±0.11	0

Supporting Information

Dewatering methanotrophic enrichments intended for single cell protein production using biomimetic aquaporin forward osmosis membranes

Borja Valverde-Pérez[a,*+], Mathias L. Pape[a+], Astrid F. Kjeldgaard[a], August A. Zachariae[a], Carina Schneider[a], Claus Hélix-Nielsen[a,b], Agata Zarebska[a], Barth F. Smets[a,*]

[a] *Department of Environmental Engineering, Technical University of Denmark, Miljøvej, Building 115, 2800 Kgs. Lyngby, Denmark (*Corresponding authors: bvape@env.dtu.dk, bfsm@env.dtu.dk)*

[b] *University of Maribor, Faculty of Chemistry and Chemical Engineering, Smetanova ulica 17, 2000 Maribor, Slovenia*

1. Salt concentration calculations for feed and draw solutions:

Table S-1 Concentrations used in the draw solutions.

		Mw	g L^{-1}		mol L^{-1}	
		[g mol^{-1}]	30 atm	60 atm	30 atm	60 atm
NaCl		58.44	81.120	157.620	1.388	2.697
$MgCl_2$		95.21	83.684	142.992	0.879	1.502
Brine	**NaCl**	58.44	70.038	132.336	1.198	2.264
	$MgCl_2$	95.21	12.951	24.471	0.136	0.257
	SUM		82.989	156.807	1.335	2.522
Glycerol		92.09	208.224	365.338	2.261	3.967

Osmotic pressure was calculated for several concentrations of each solute by measuring osmolarity at 20 °C and using the van't Hoff equation:

$$\pi = i \cdot \mathrm{M} \cdot \mathrm{R} \cdot \mathrm{T}$$

Where M is the concentration of the solute (mol L^{-1}), R is the ideal gas constant (atm L mol^{-1} K^{-1}), T is the temperature (K) and i is the van't Hoff factor. Osmolarity, which was experimentally determined, can be estimated as:

$$osmolarity = \sum_j M_j \cdot i_j$$

Thus, regression curves were built where the concentration of each solute was correlated with osmotic pressure, based on which the solutes concentrations to reach 30 and 60 bars were chosen.

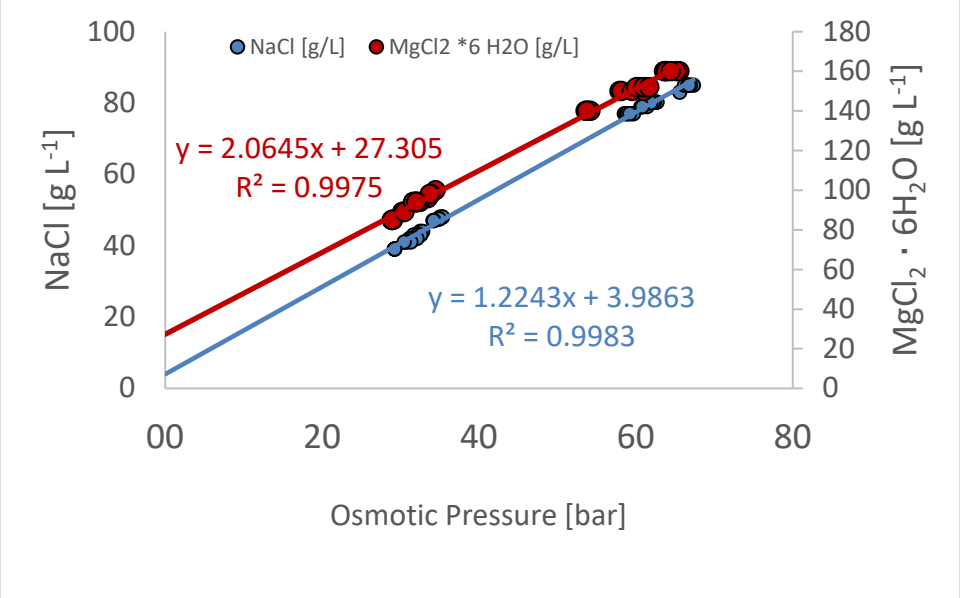

Figure S-1 Correlation between salt concentration and osmotic pressure.

Salt concentrations in the FS, used to estimate solute back fluxes, was calculated from the conductivity measurements using the following empirical correlations:

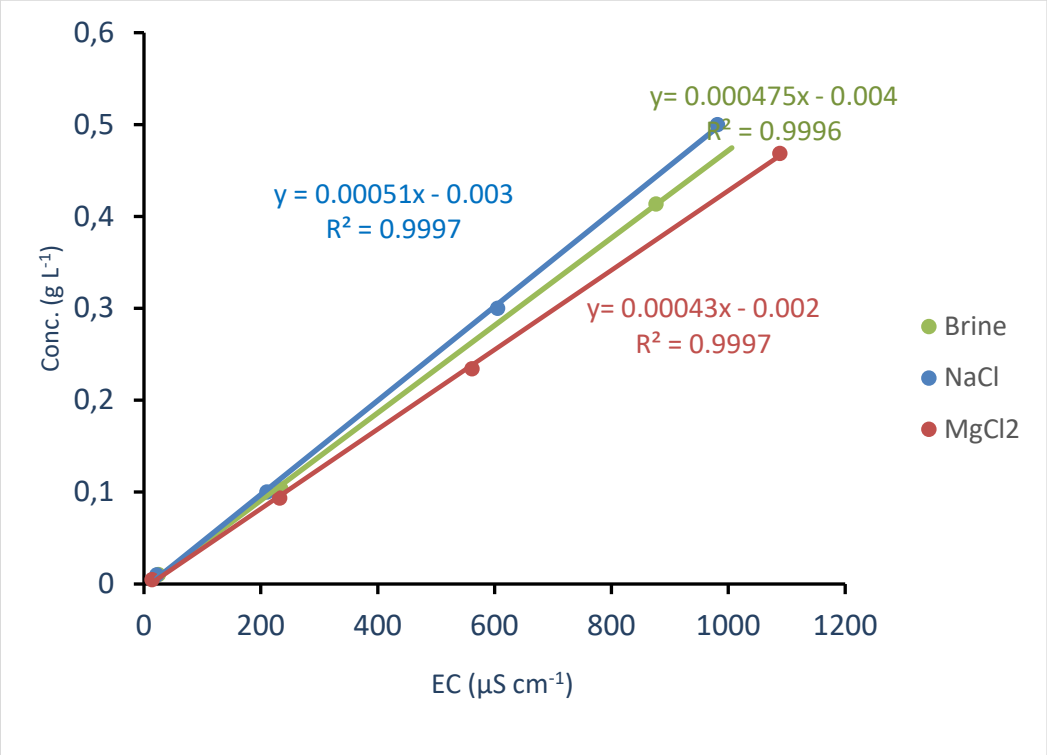

Figure S-2 Correlation between salt concentration and conductivity.

2. dAMS media composition:

Table S-2 dAMS media composition.

dAMS medium (25 mg NH_4^+-N / L)
Stock A: $MgSO_4$ x $7H_2O$ 10.0 g NH_4Cl 5.0 g $CaCl_2$ x $2H_2O$ 1.5 g Distilled water 1 L **FeNaEDTA stock:** FeNaEDTA 0.5 g Distilled water 100 mL **Na_2HPO_4 stock:** Na_2HPO_4 x $12H_2O$ 71.7 g Distilled water 1 L **KH_2PO_4 stock:** KH_2PO_4 27.2 g Distilled water 1 L **1000x trace solution:** Na_2EDTA x $2H_2O$ 0.5 g $FeSO_4$ x $7H_2O$ 0.2 g H_3BO_3 0.03 g $CoCl_2$ x $6H_2O$ 0.02 g $ZnSO_4$ x $7H_2O$ 0.01 g $MnCl_2$ x $4H_2O$ 0.003 g Na_2MoO_4 x $2H_2O$ 0.003 g $NiCl_2$ x 6H2O 0.002 g $CuSO_4$ x $5H_2O$ 0.025 g Distilled water 1 L **dAMS medium:** Dilute 20 mL of Stock A to 800 mL. Add 1 mL FeNaEDTA Stock and 1 mL trace solution. Dissolve and bring to 1 liter (distilled water) After sterilization, cool to 50 °C – 60 °C and add first 25 mL KH_2PO_4 Stock (filter sterilized) followed by 25 mL Na_2HPO_4

Stock (filter sterilized). pH of the medium should be 6.8

3. Correlation between OD_{600} and total suspended solids:

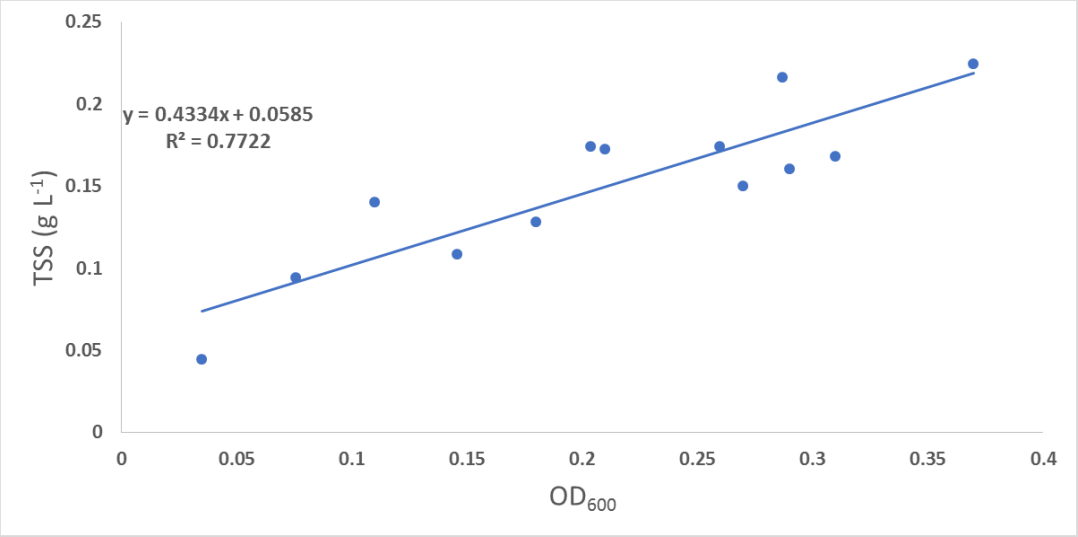

Figure S-3Correlation between OD_{600} and total suspended solids.

4. Experimental data from 24 hours batches for FO performance characterization and further data treatment:

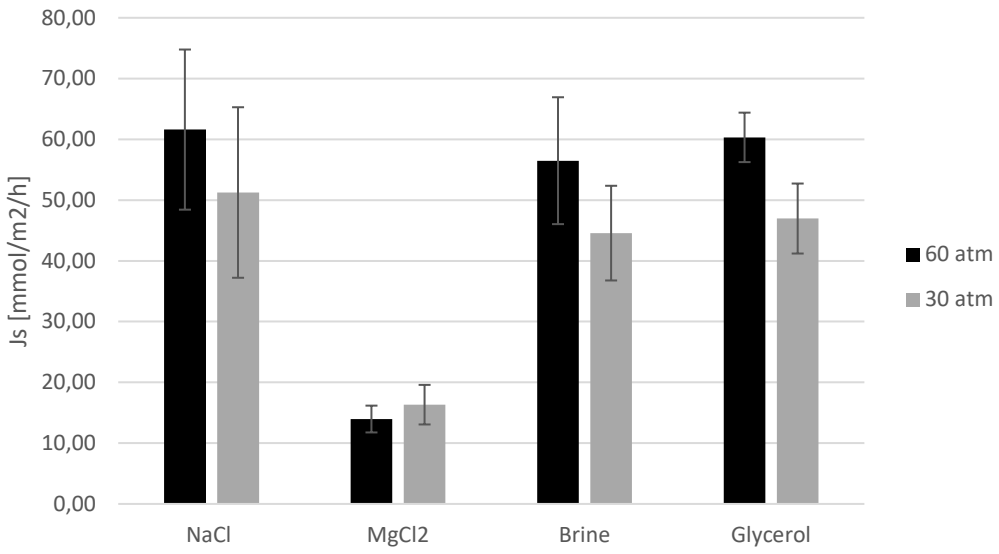

Figure S-4 Molar reverse flux of draw solution solutes in the experiments with milli-Q water as feed solution.

Table S-3 Normalized NH_3 rejection during biofouling experiments.

Exp #			Mean	STD
11	$MgCl_2$	30	62.0%	7.7%
12	$MgCl_2$	60	62.9%	4.9%
13	NaCl	60	7.9%	28.1%
14	NaCl	30	-17.9%	3.7%
14	Glycerol	30	100%	0.3%
16	Brine	30	4.7%	9.6%

Table S-4 pH in the feed (FS) and draw solutions (DS) at the start and end of FO experiments in setups A and B, which are identical.

		FS				DS			
		A		B		A		B	
		Start	End	Start	End	Start	End	Start	End
Exp #	**MilliQ water as FS**								
1	NaCl, 30 bar	6.48	6.22	6.51	6.82	5.79	5.46	5.75	5.68
2	NaCl, 60 bar	6.52	6.38	6.31	7.05	6.05	5.83	6.14	5.94
3	$MgCl_2$, 30 bar	6.5	5.61	6.53	6.76	5.18	5.21	4.99	5.38
4	$MgCl_2$, 60 bar	6.63	5.82	6.75	6.88	5.23	4.48	5.26	5.42
5	Brine, 30 bar	6.58	6.2	6.53	6.7	5.6	5.33	5.59	5.56
6	Brine, 60 bar	6.82	6.33	6.47	6.67	5.44	5.23	5.44	5.58
7	Glycerol, 30 bar	5.82	5.44	5.69	6.18	5.08	5.28	5.18	5.65
8	Glycerol, 60 bar	6.41	5.8	5.93	6.45	6.05	5.66	6.16	5.57
	Ammonium solution as FS								
9	Brine, 30 bar	5.79	5.52	6.09	5.73	5.50	5.09	5.38	5.24
10	Glycerol, 60 bar	**n.a.**	**n.a.**	**n.a.**	**n.a.**	**n.a.**	**n.a.**	**n.a.**	**n.a.**
	Active methanotrophic culture as FS								
11	NaCl, 30 bar	6.50	6.07	6.50	6.38	5.39	5.12	5.39	5.84
12	NaCl, 60 bar	6.96	6.50	6.96	6.28	5.56	5.90	5.65	5.85
13	$MgCl_2$, 30 bar	6.84	6.13	6.84	6.57	5.27	5.85	5.18	5.63
14	$MgCl_2$, 60 bar	6.95	6.47	6.95	6.76	5.37	5.66	5.32	5.51
15	Brine, 30 bar	6.60	6.08	6.60	6.21	5.13	4.19	5.42	5.14
16	Glycerol, 30 bar	6.81	6.39	6.81	6.67	5.48	6.15	5.34	5.84

Table S-5 Biomass concentrations at the beginning and end of the FO experiments.

Experiment		TSS (g L^{-1})		OD_{600}		Growth rate (d^{-1})	
		Start	End	Start	End	Mean	STD
11	NaCl, 30 atm	0.05	0.15	0.14	0.36	0.91	0.34
12	NaCl, 60 atm	0.09	0.20	0.23	0.48	0.72	0.18
13	$MgCl_2$, 30 atm	0.02	0.11	0.07	0.31	1.41	0.35
14	$MgCl_2$, 60 atm	n.a.	n.a.	0.11	0.32	1.07	0.36
15	Brine, 30 atm	0.07	0.18	0.15	0.36	0.85	0.07
16	Glycerol, 30 atm	0.06	0.14	0.13	0.28	0.71	0.52

Table S-6 Concentration factors for biofouling experiments.

Experiments	**Concentration Factor**
11	1.59±0.06
12	1.78±0.02
13	1.94±0.14
14	1.49±0.03
15	1.81±0.05
16	1.76±0.05

Water fluxes and solute back fluxes for all experiments estimated as 30 min averages (from 6 data collected with 5 min frequency). Js is not reported for glycerol experiments was estimated based on the initial and final glycerol concentration in the feed solution and thus not reported in the following figures.

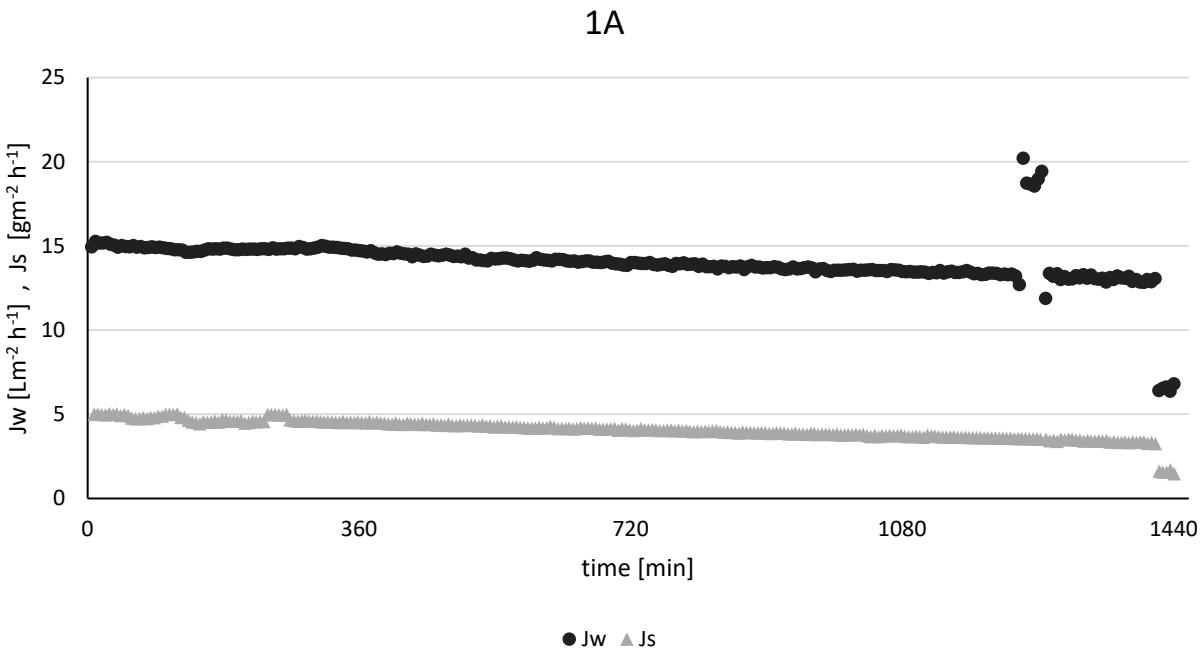

Figure S-5 Water flux (J_w) and solute back flux (J_s) during experiment 1 duplicate A.

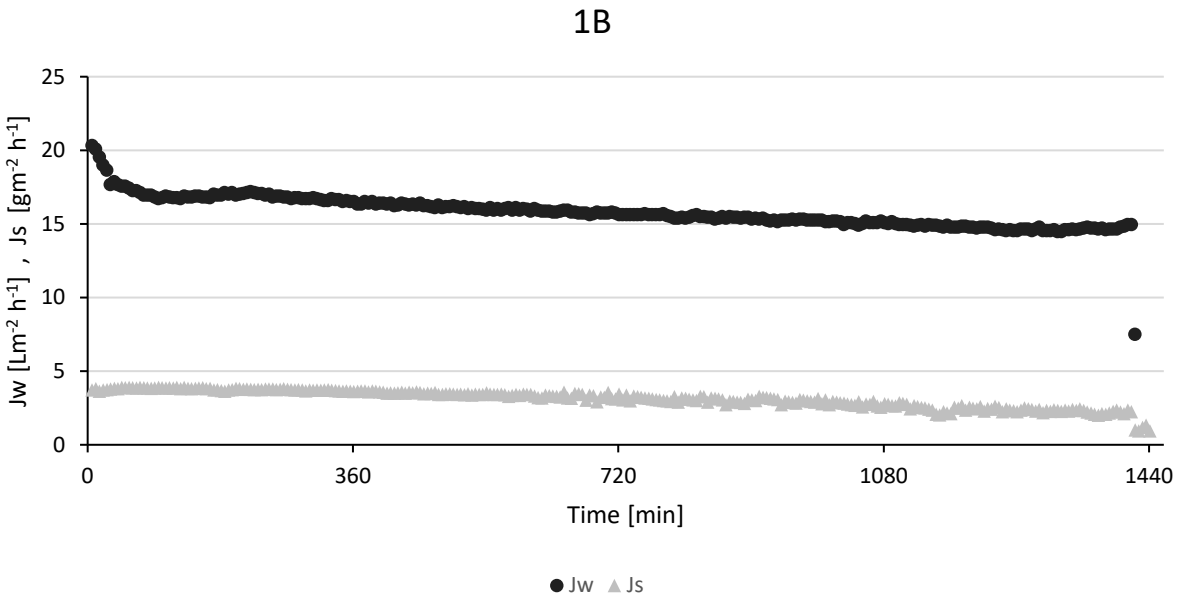

Figure S-6 Water flux (J_w) and solute back flux (J_s) during experiment 1 duplicate B.

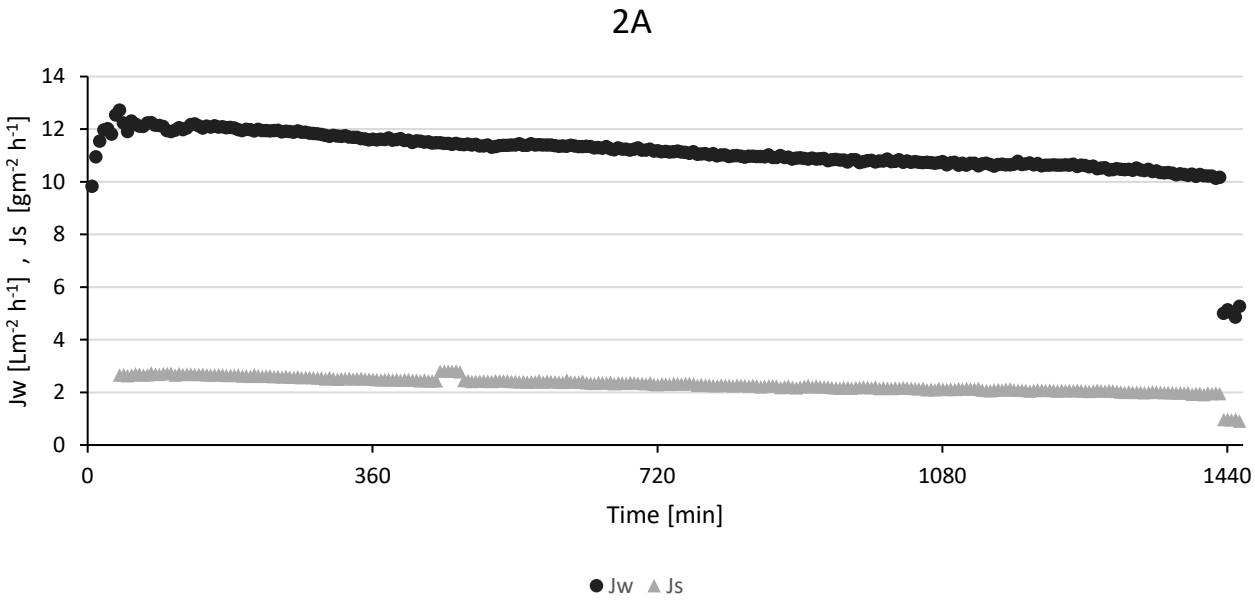

Figure S-7 Water flux (J_w) and solute back flux (J_s) during experiment 2 duplicate A.

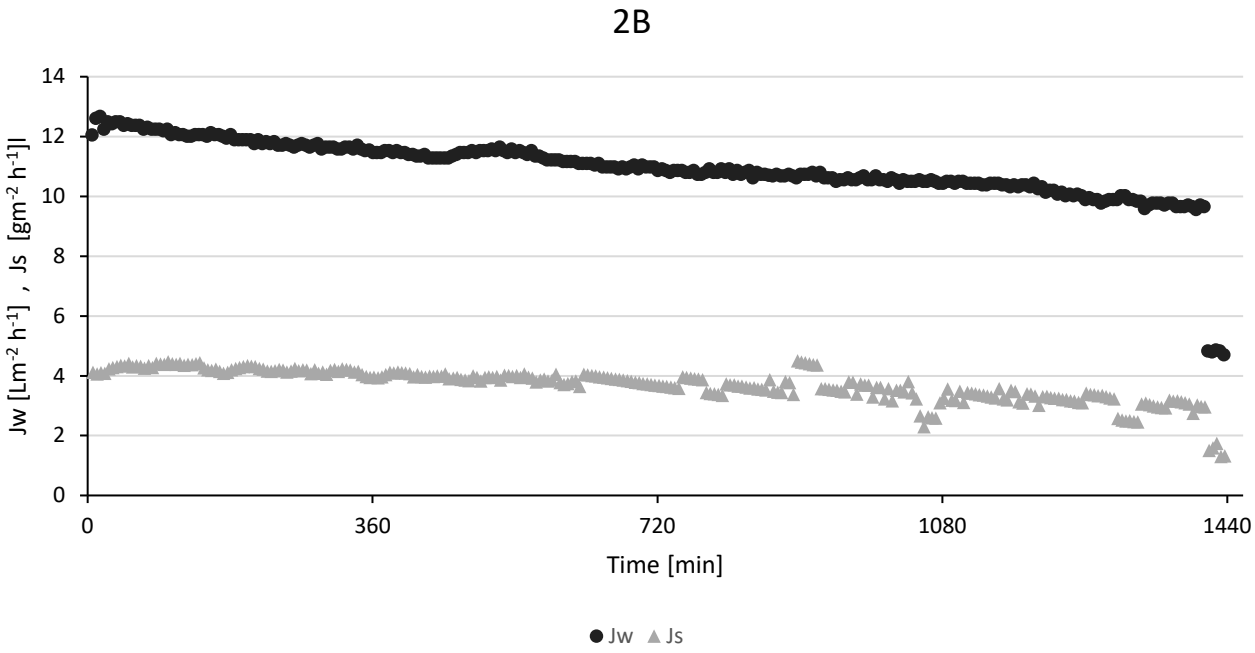

Figure S-8 Water flux (J_w) and solute back flux (J_s) during experiment 2 duplicate B.

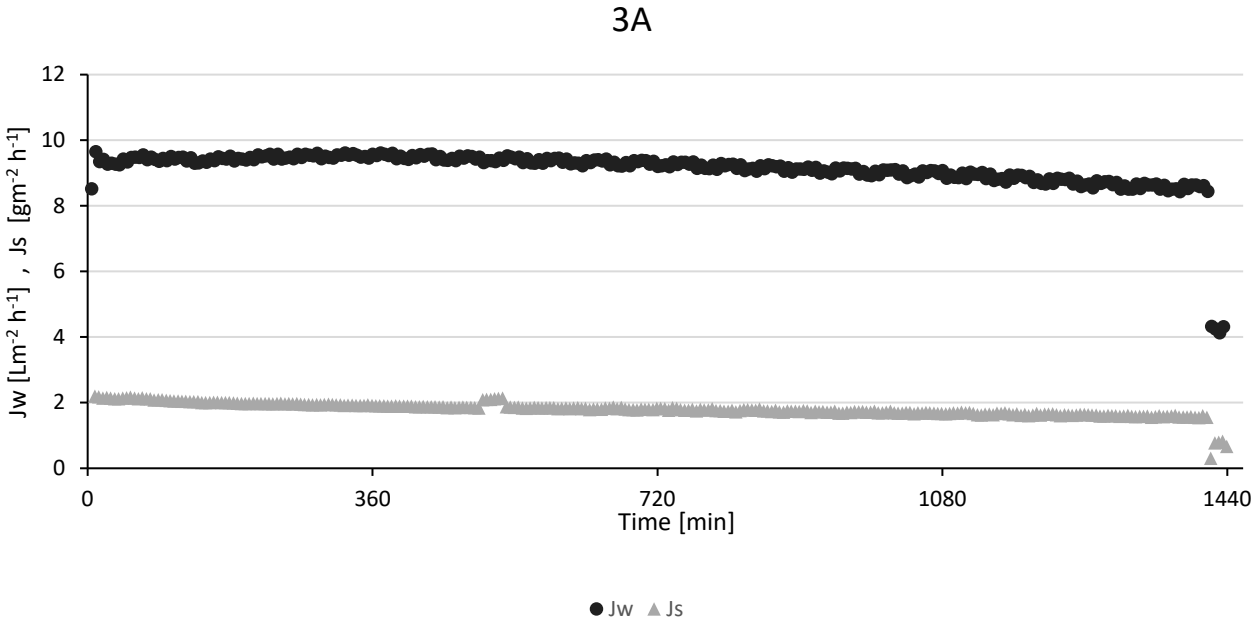

Figure S-9 Water flux (J_w) and solute back flux (J_s) during experiment 3 duplicate A.

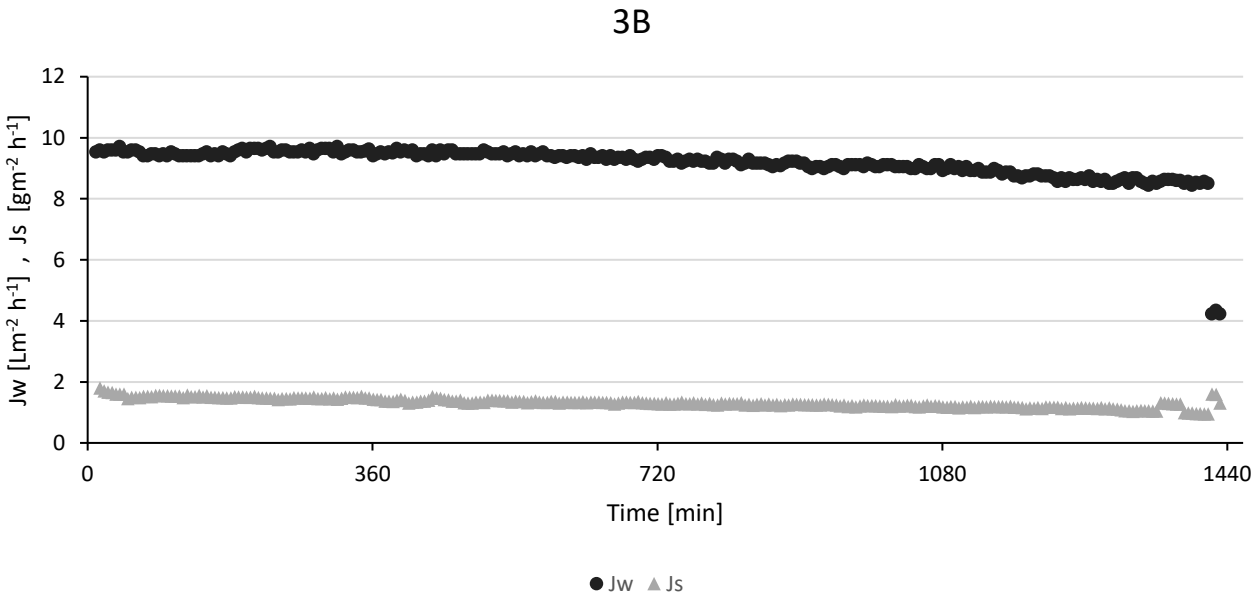

Figure S-10 Water flux (J_w) and solute back flux (J_s) during experiment 3 duplicate B.

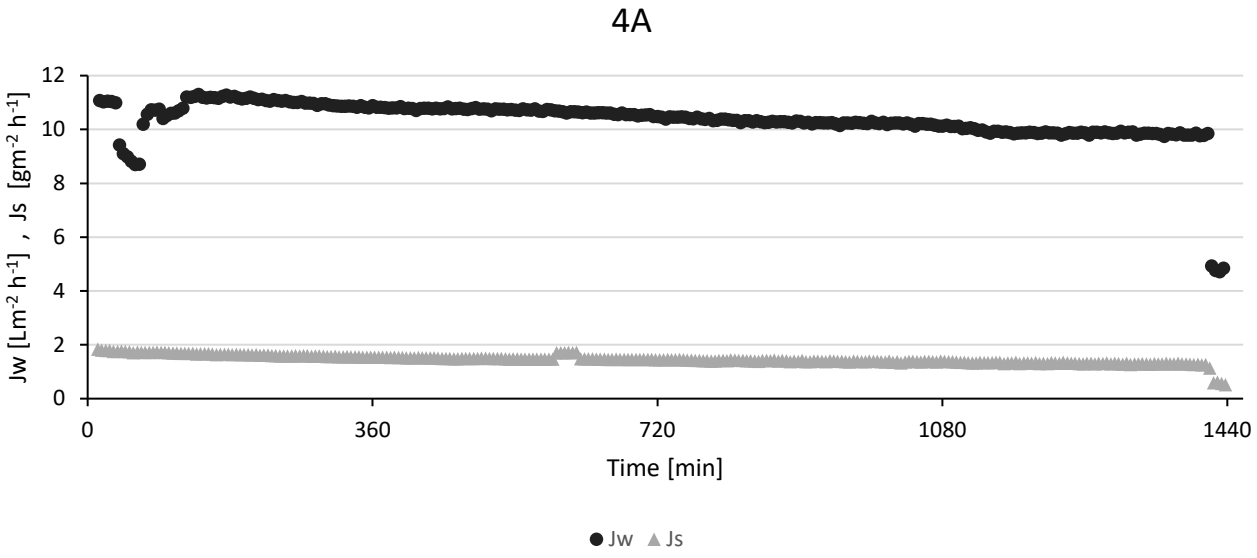

Figure S-11 Water flux (J_w) and solute back flux (J_s) during experiment 4 duplicate A.

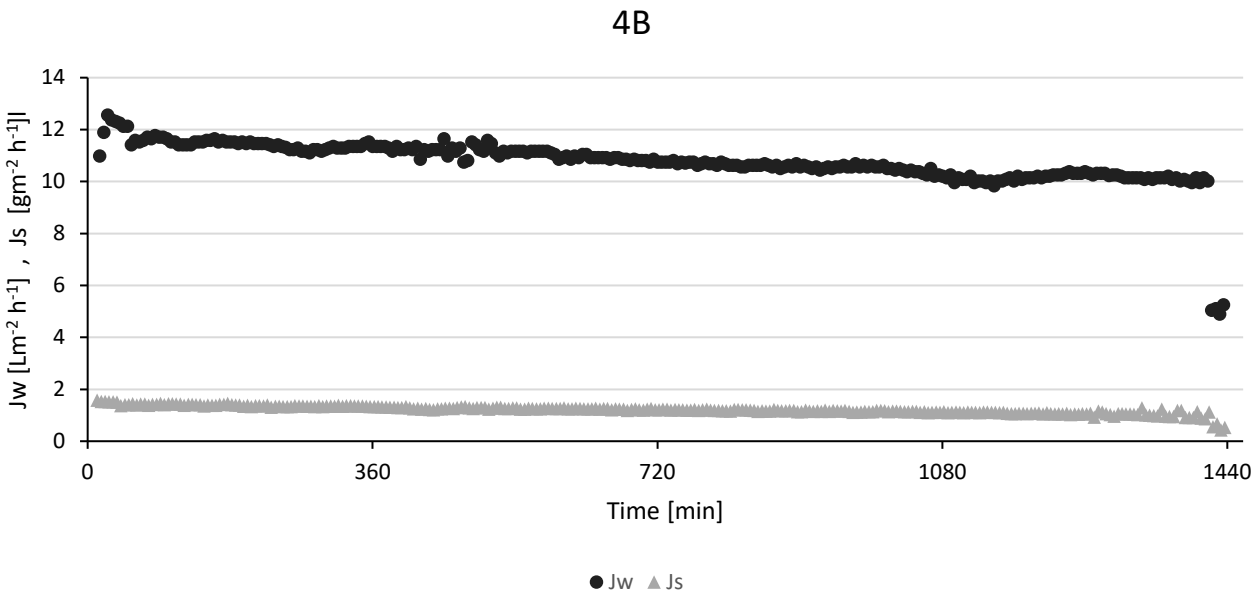

Figure S-12 Water flux (J_w) and solute back flux (J_s) during experiment 4 duplicate B.

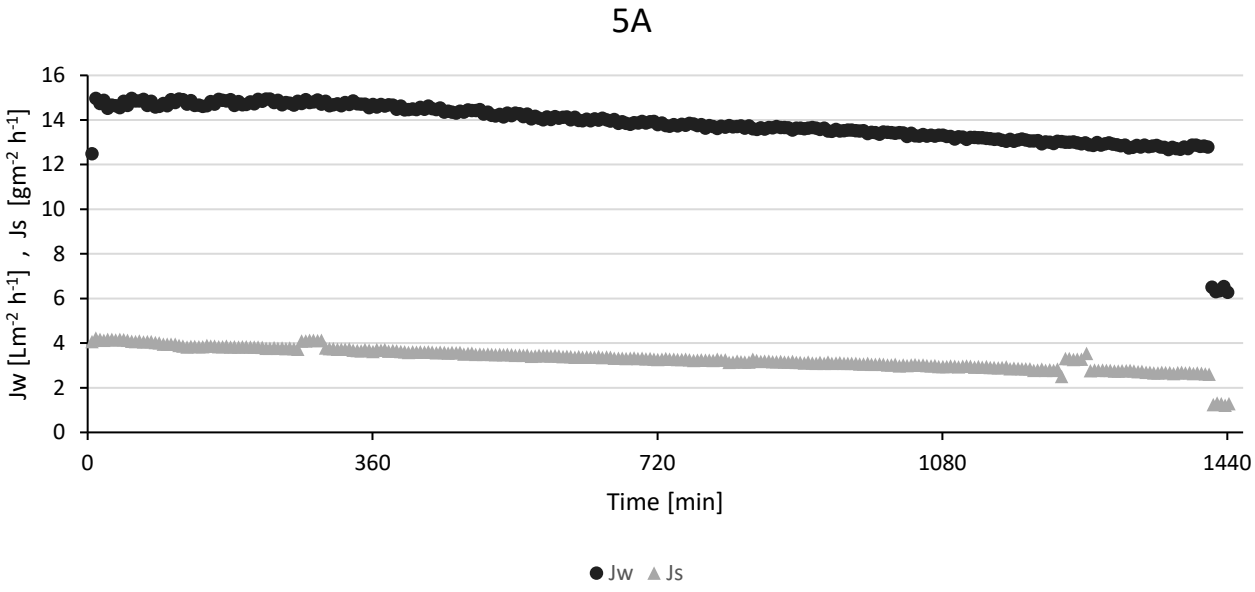

Figure S-13 Water flux (J_w) and solute back flux (J_s) during experiment 5 duplicate A.

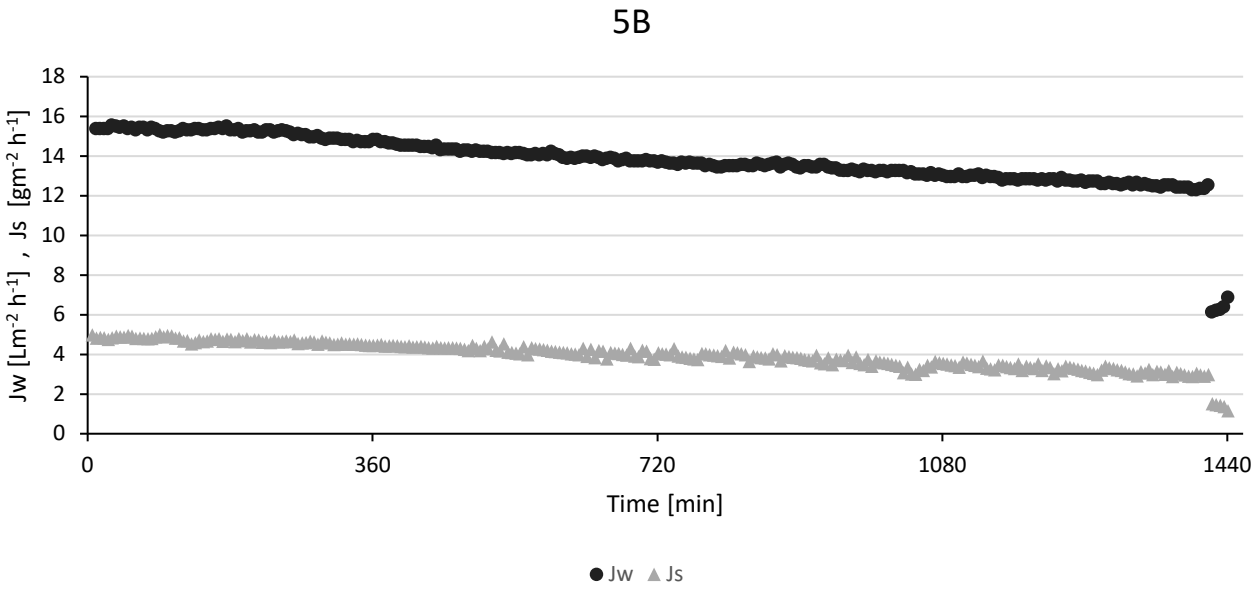

Figure S-14 Water flux (J_w) and solute back flux (J_s) during experiment 5 duplicate B.

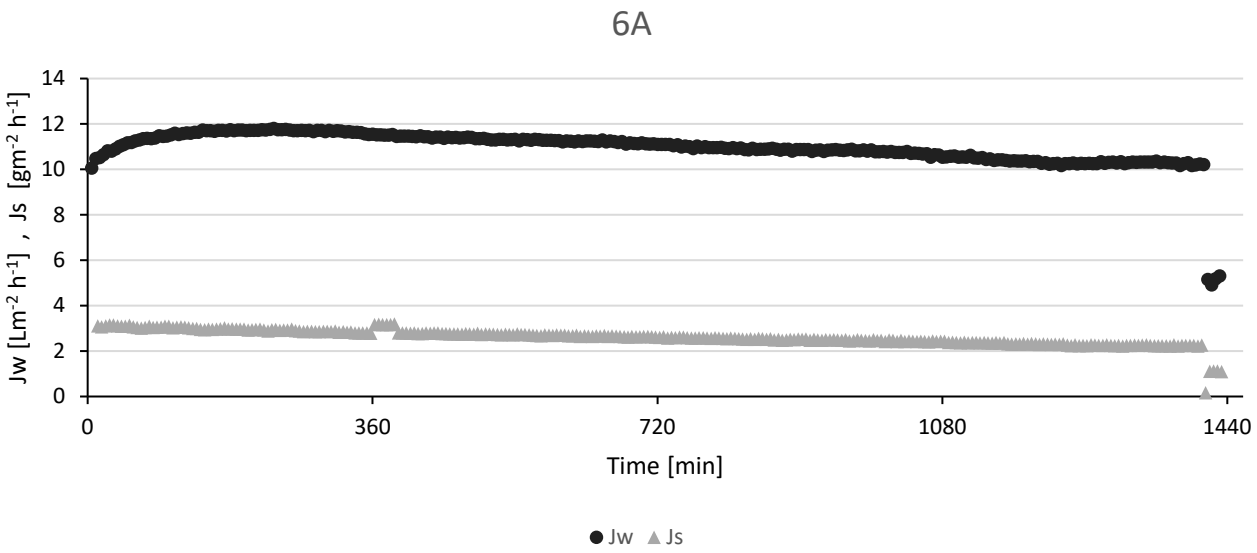

Figure S-15 Water flux (J_w) and solute back flux (J_s) during experiment 6 duplicate A.

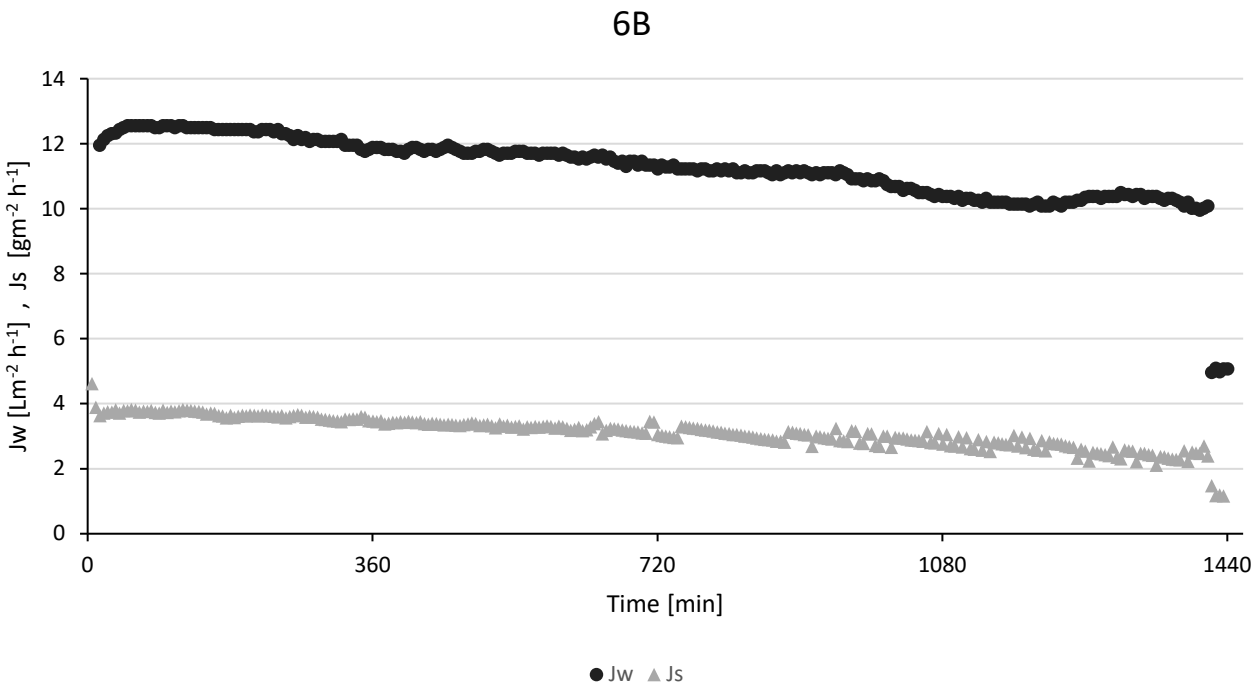

Figure S-16 Water flux (J_w) and solute back flux (J_s) during experiment 6 duplicate B.

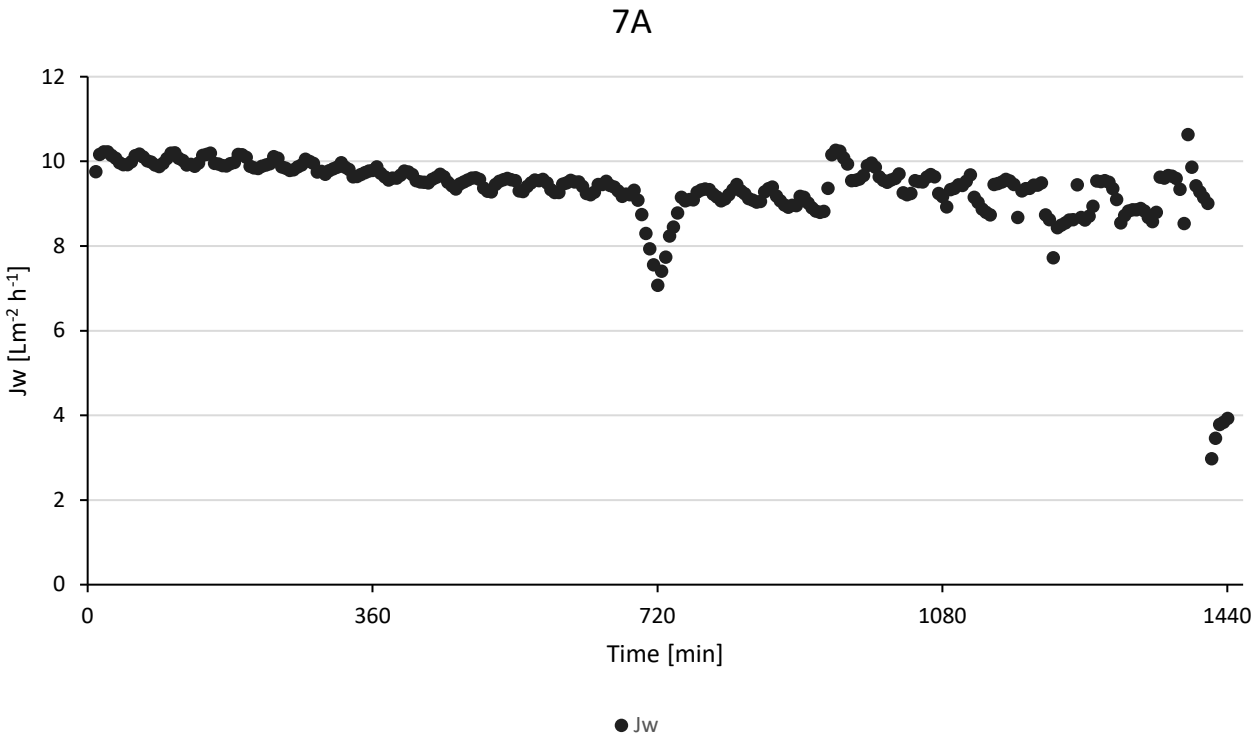

Figure S-17 Water flux (J_w) and solute back flux (J_s) during experiment 7 duplicate A.

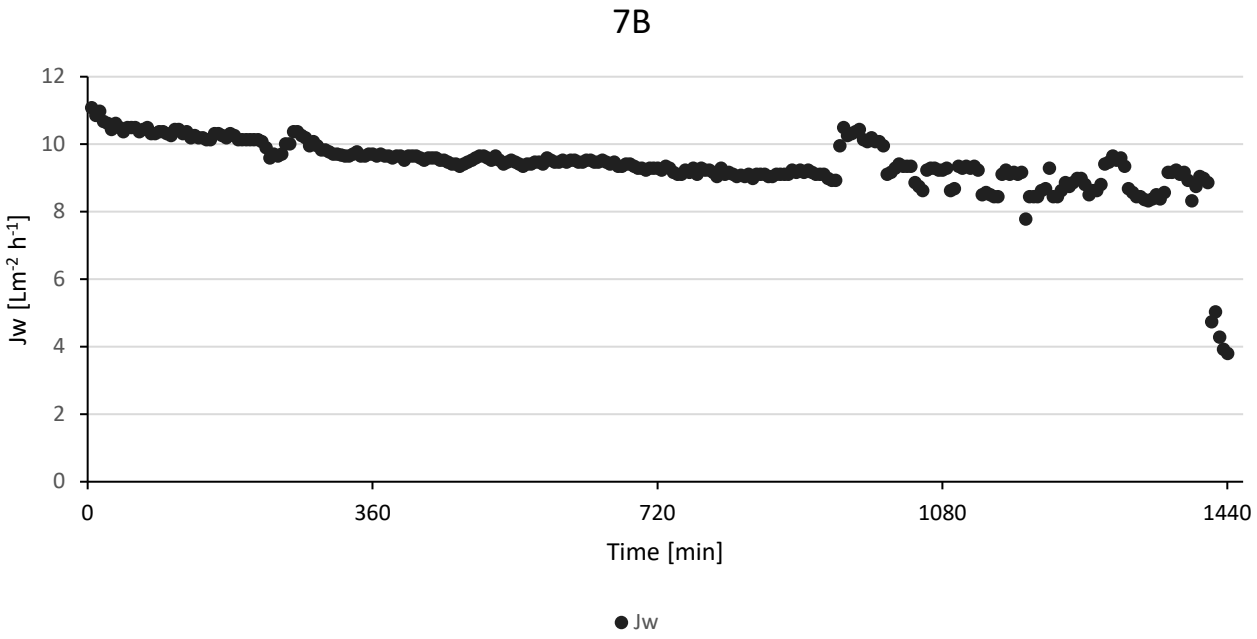

Figure S-18 Water flux (J_w) and solute back flux (J_s) during experiment 7 duplicate B.

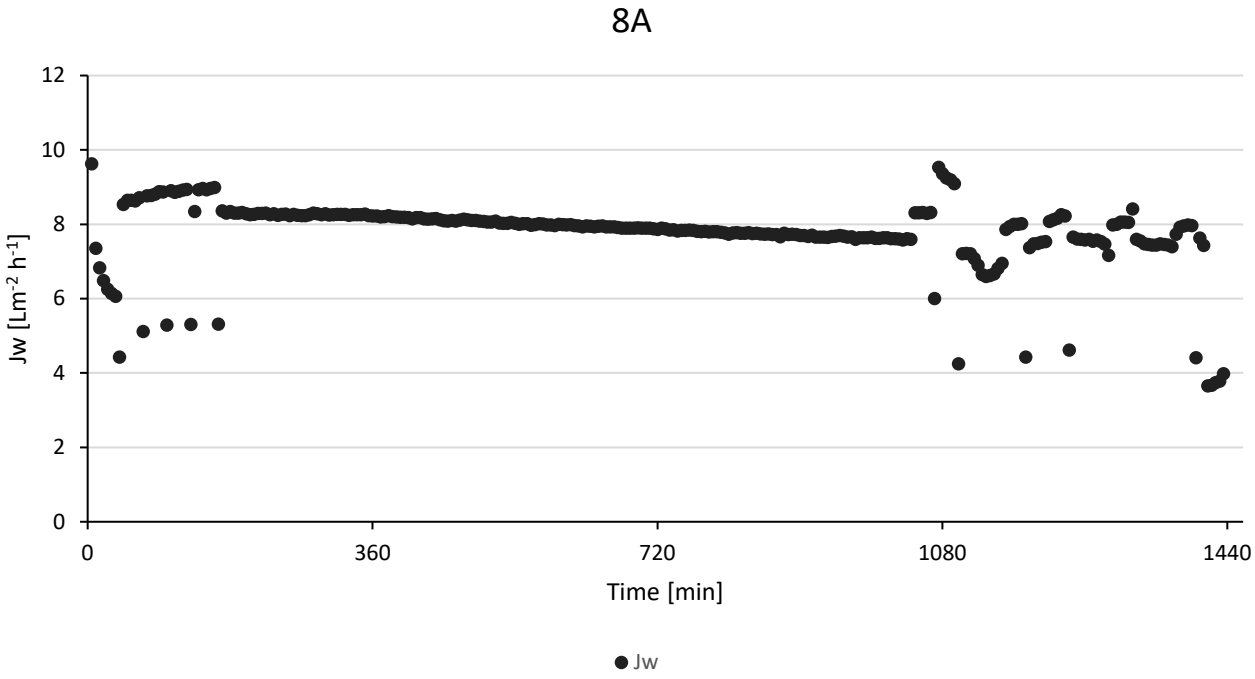

Figure S-19 Water flux (J_w) and solute back flux (J_s) during experiment 8 duplicate A.

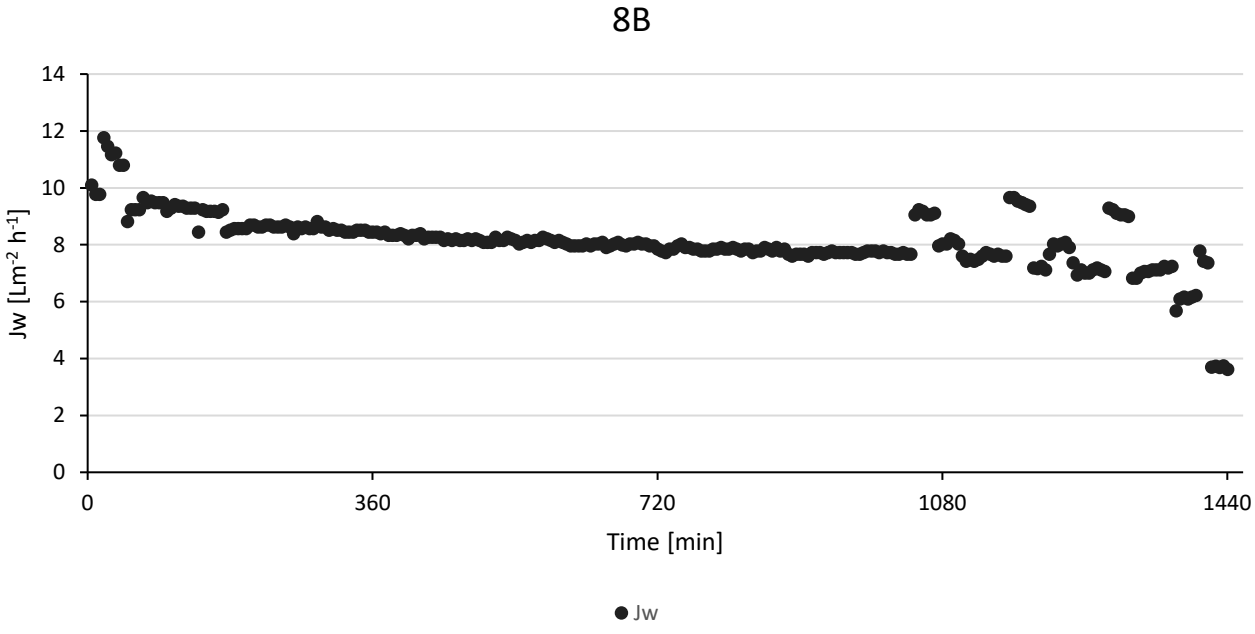

Figure S-20 Water flux (J_w) and solute back flux (J_s) during experiment 8 duplicate B.

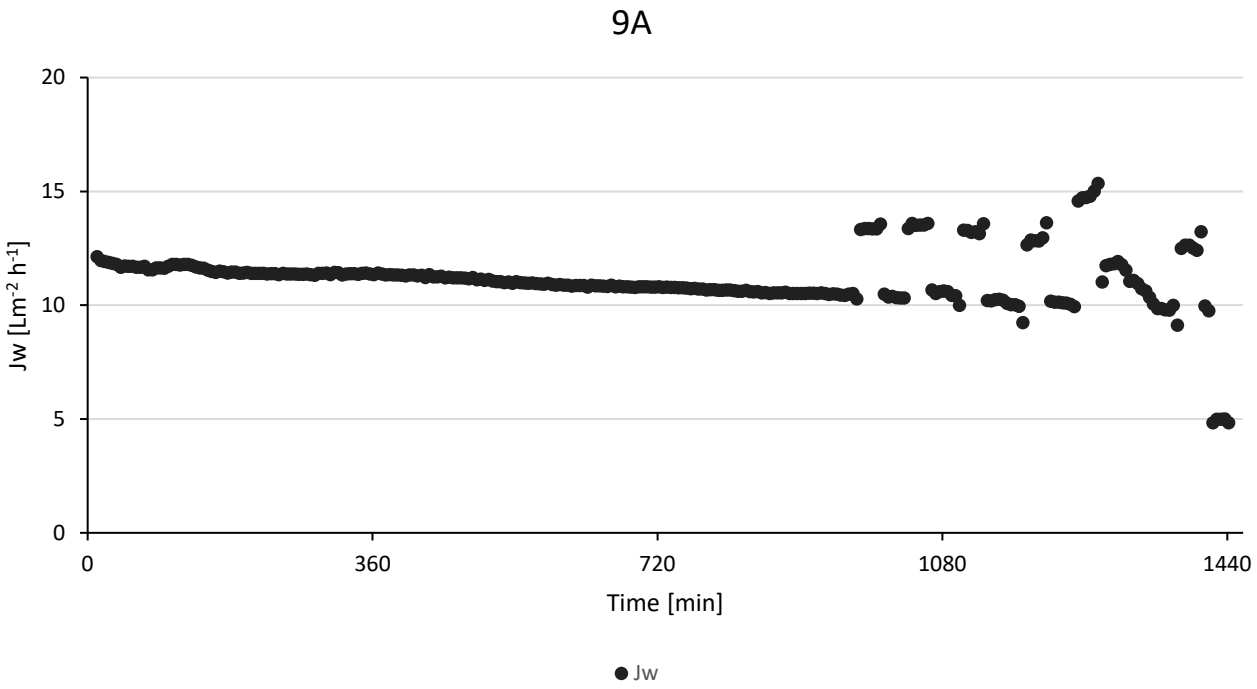

Figure S-21 Water flux (J_w) and solute back flux (J_s) during experiment 9 duplicate A.

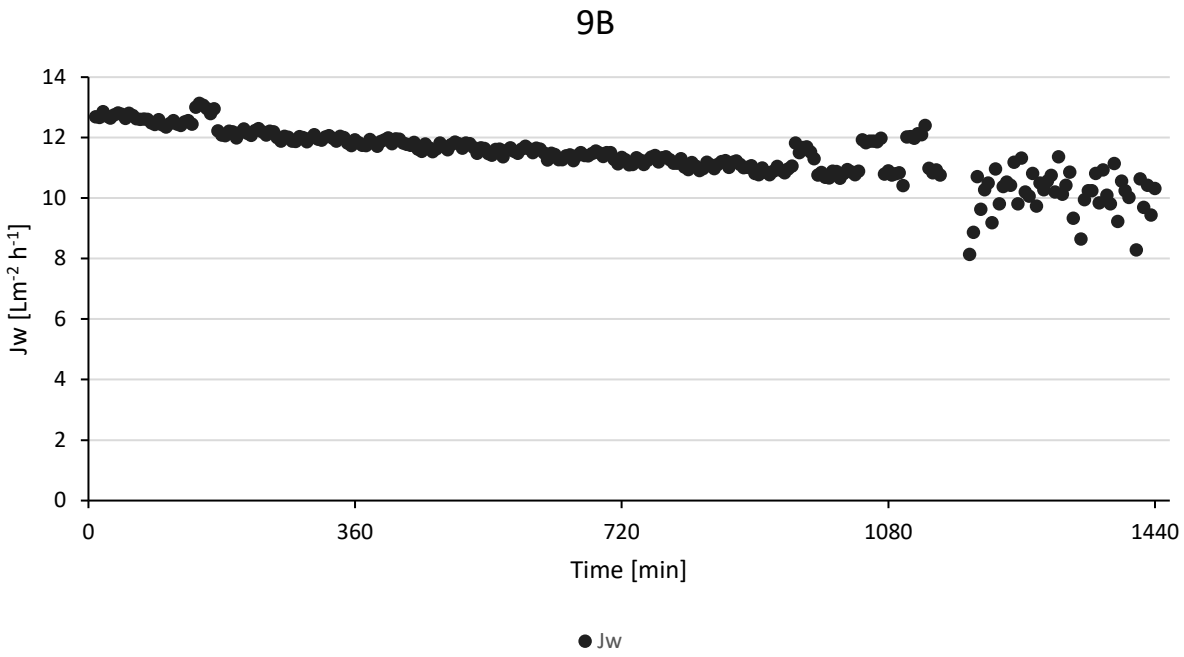

Figure S-22 Water flux (J_w) and solute back flux (J_s) during experiment 9 duplicate B.

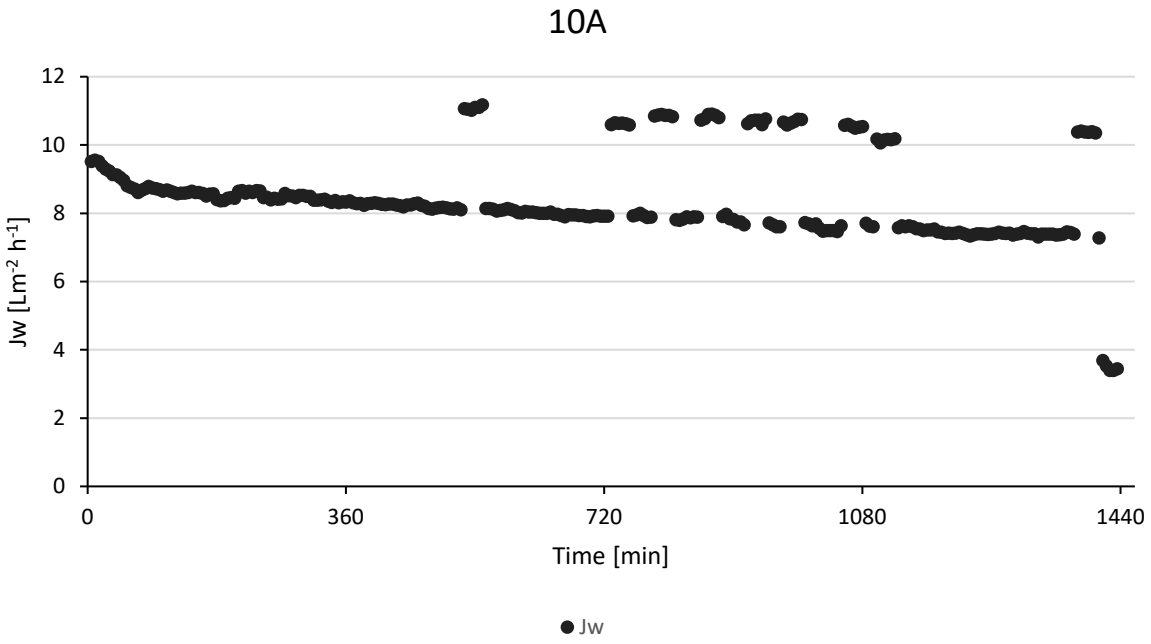

Figure S-23 Water flux (J_w) and solute back flux (J_s) during experiment 10 duplicate A.

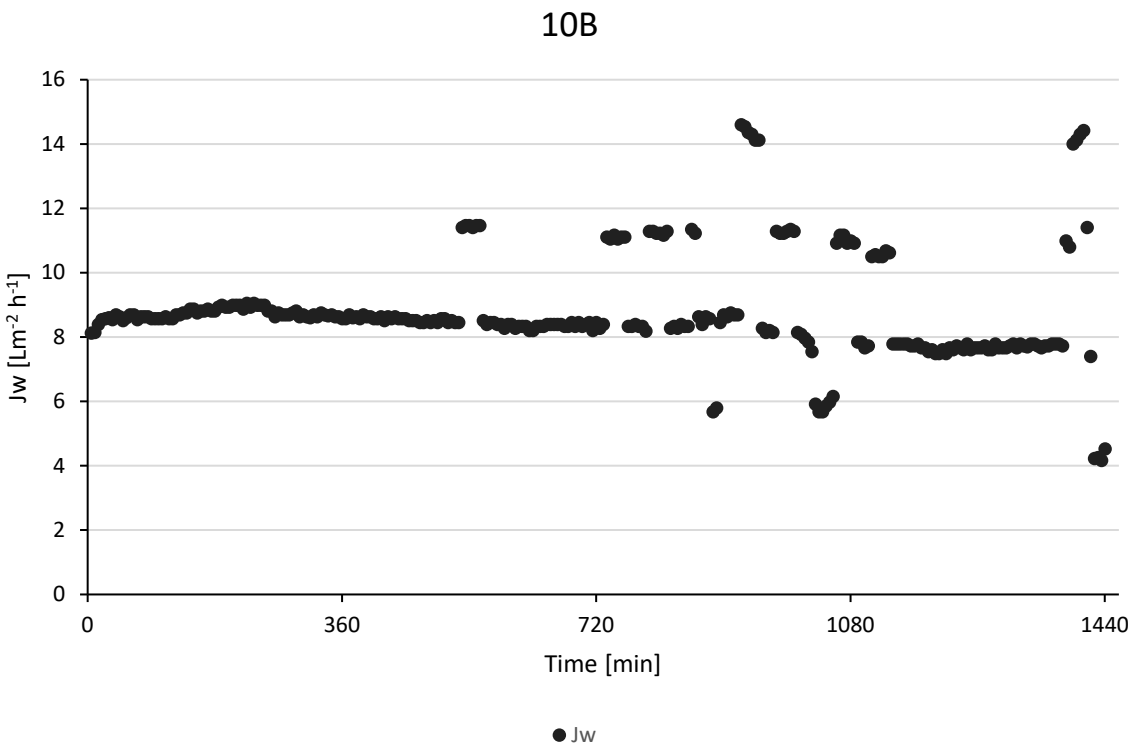

Figure S-24 Water flux (J_w) and solute back flux (J_s) during experiment 10 duplicate B.

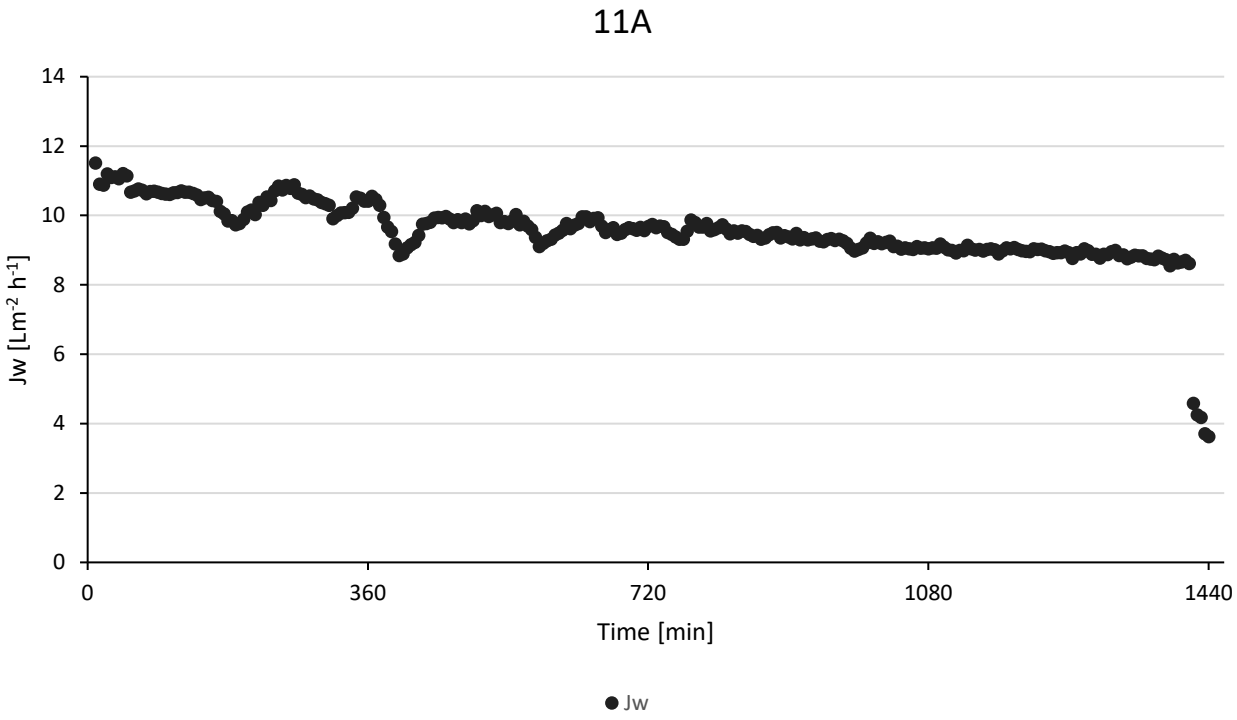

Figure S-25 Water flux (J_w) and solute back flux (J_s) during experiment 11 duplicate B.

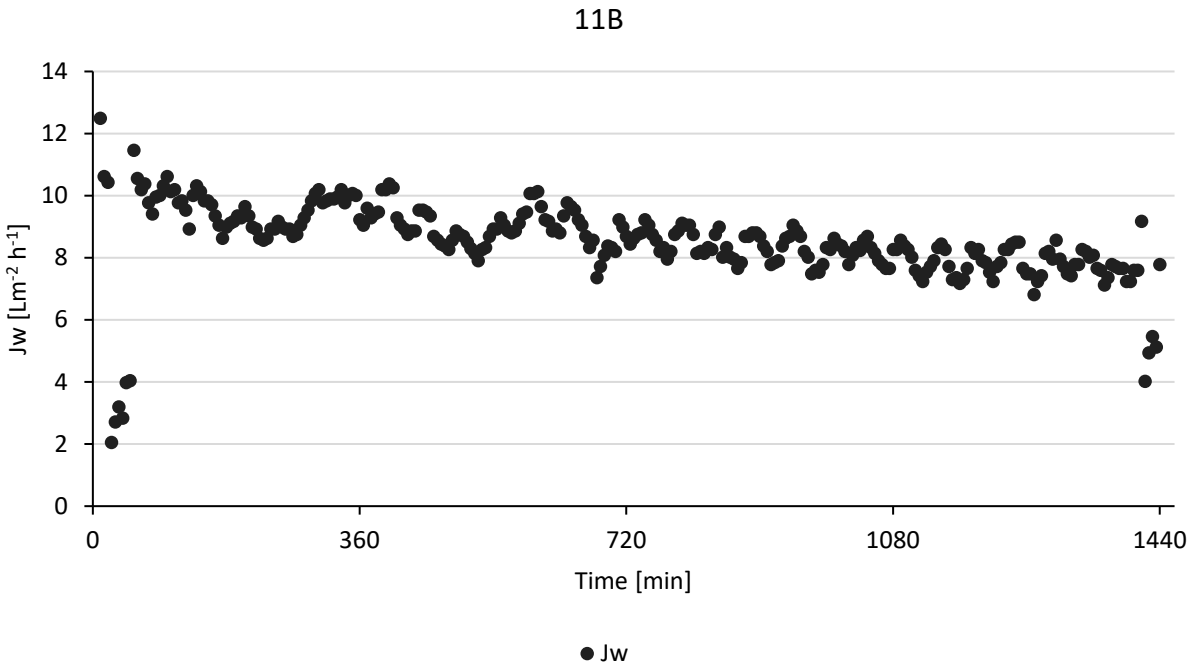

Figure S-26 Water flux (J_w) and solute back flux (J_s) during experiment 11 duplicate B.

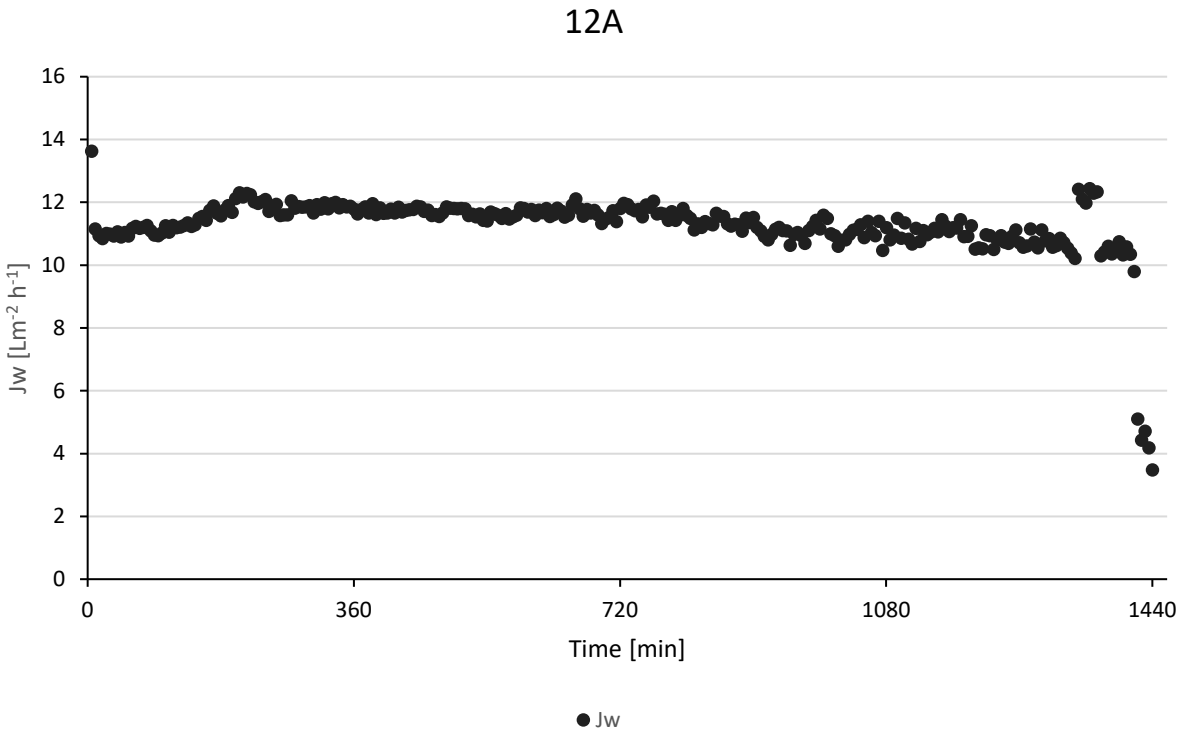

Figure S-27 Water flux (J_w) and solute back flux (J_s) during experiment 12 duplicate A.

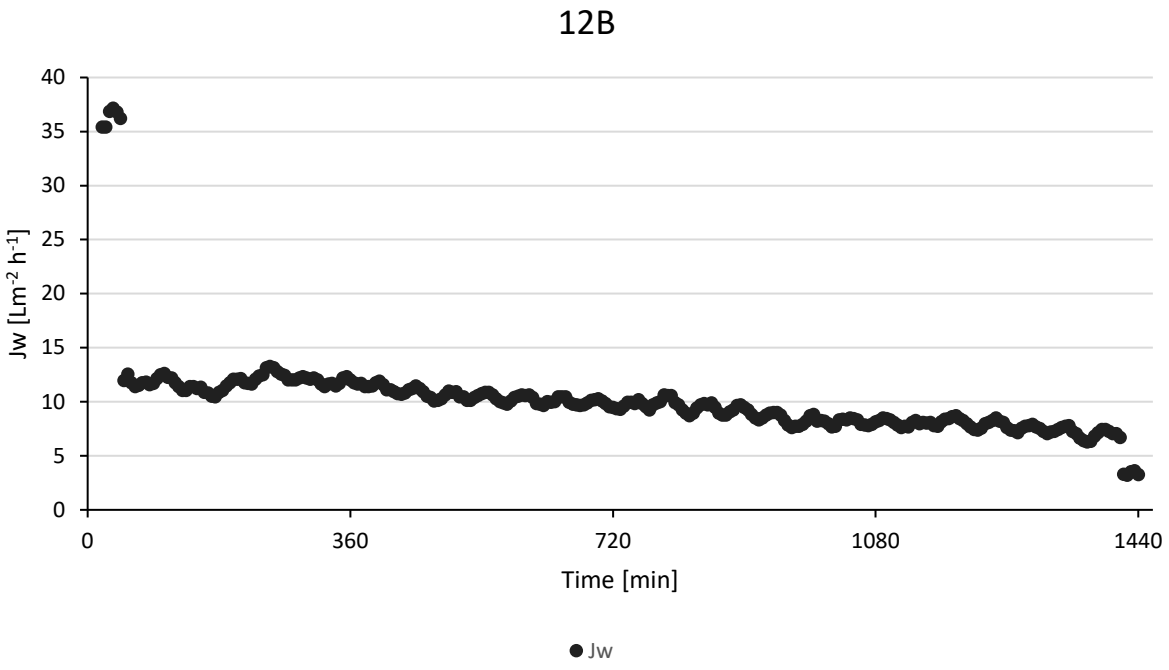

Figure S-28 Water flux (J_w) and solute back flux (J_s) during experiment 12 duplicate B.

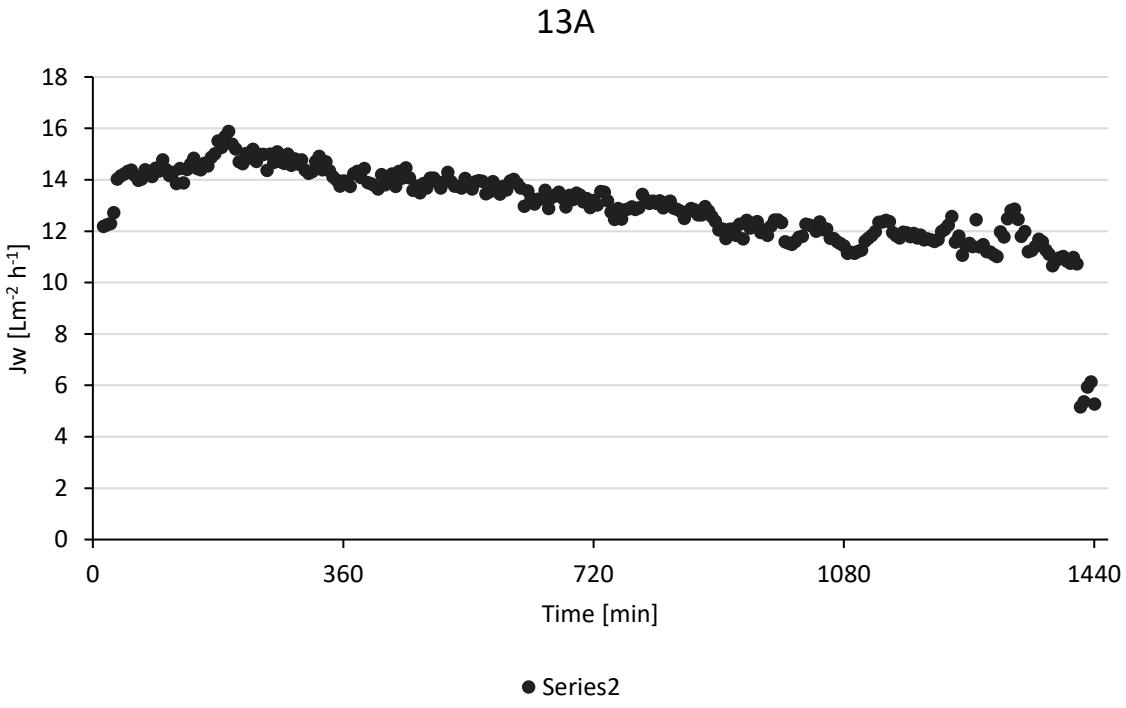

Figure S-29 Water flux (J_w) and solute back flux (J_s) during experiment 13 duplicate A.

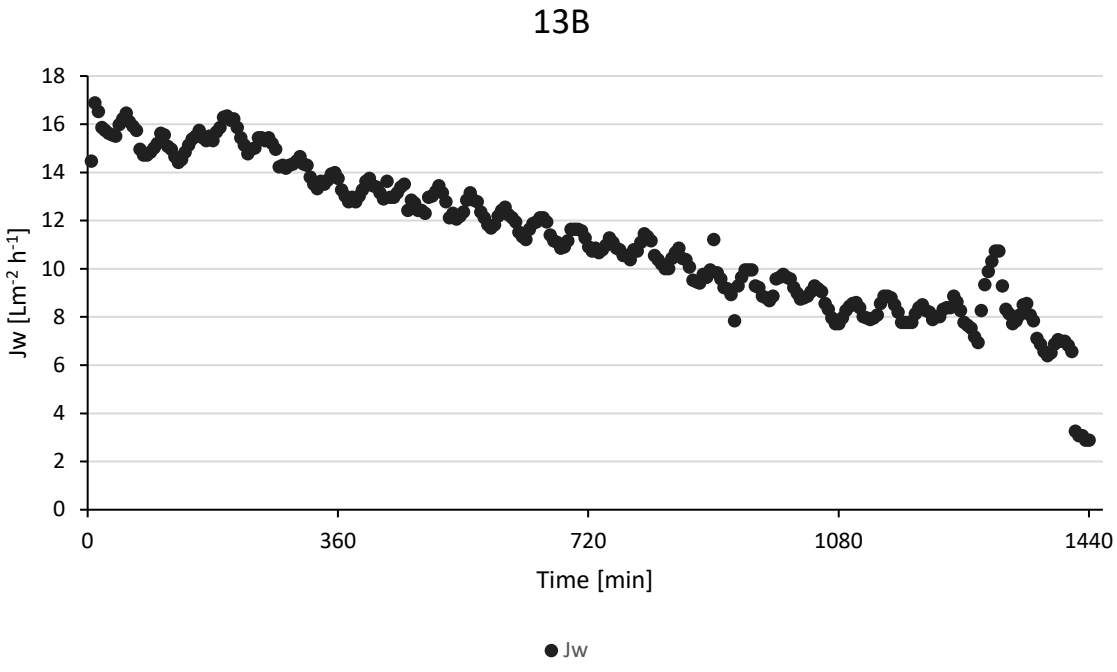

Figure S-30 Water flux (J_w) and solute back flux (J_s) during experiment 13 duplicate B.

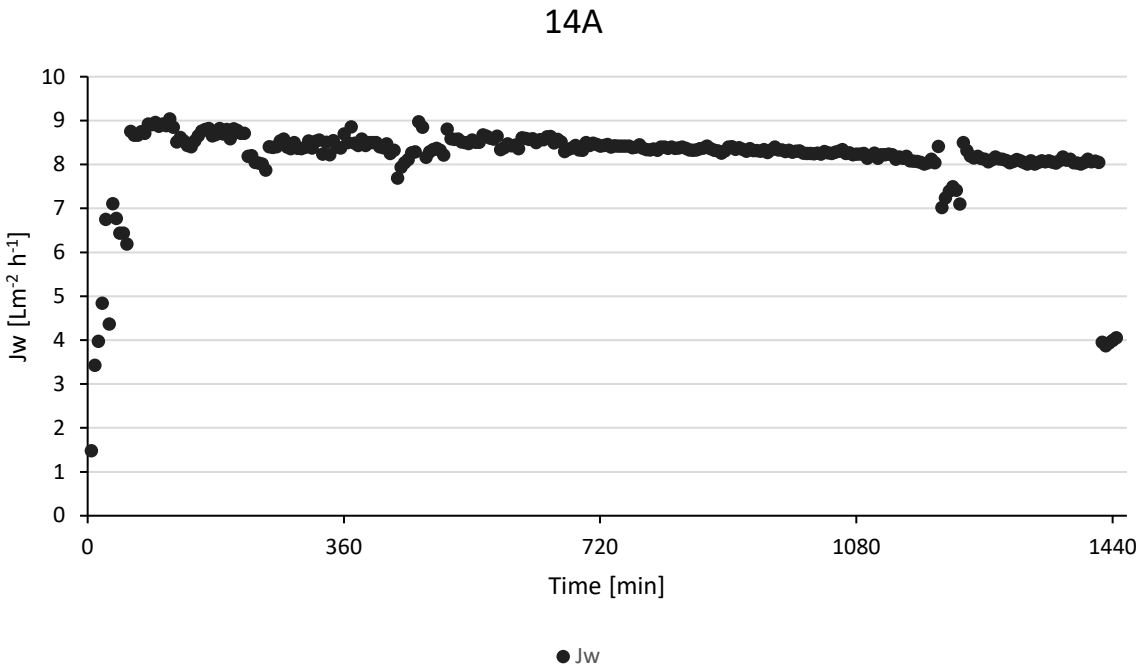

Figure S-31 Water flux (J_w) and solute back flux (J_s) during experiment 14 duplicate A.

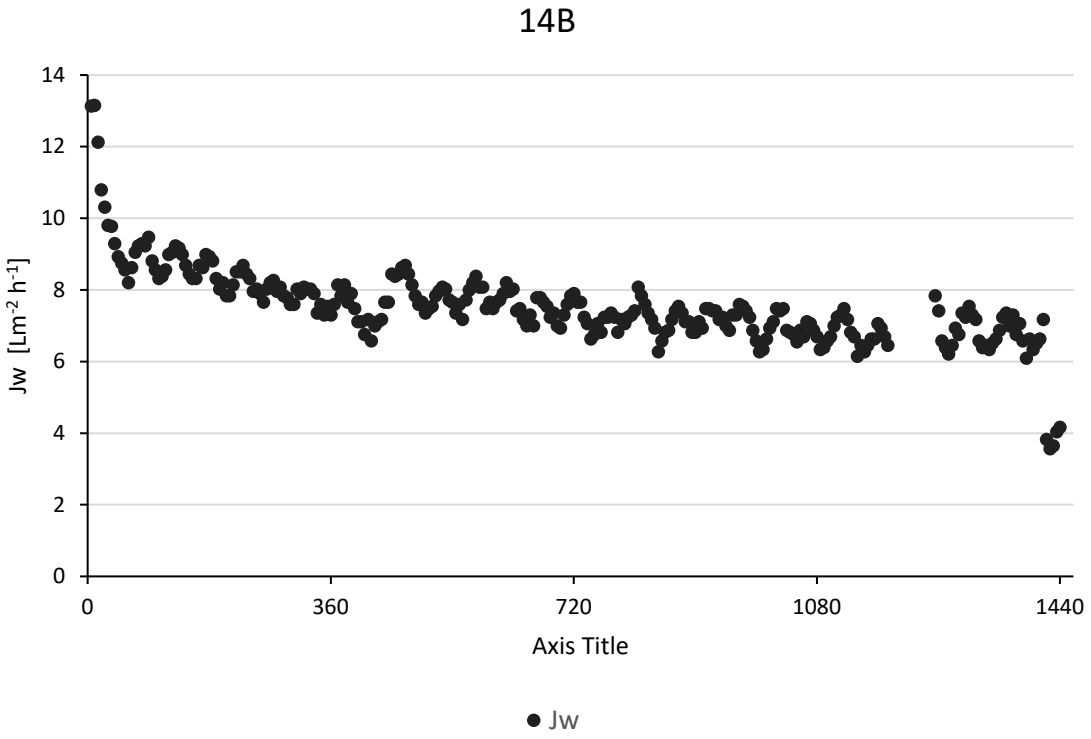

Figure S-32 Water flux (J_w) and solute back flux (J_s) during experiment 14 duplicate B.

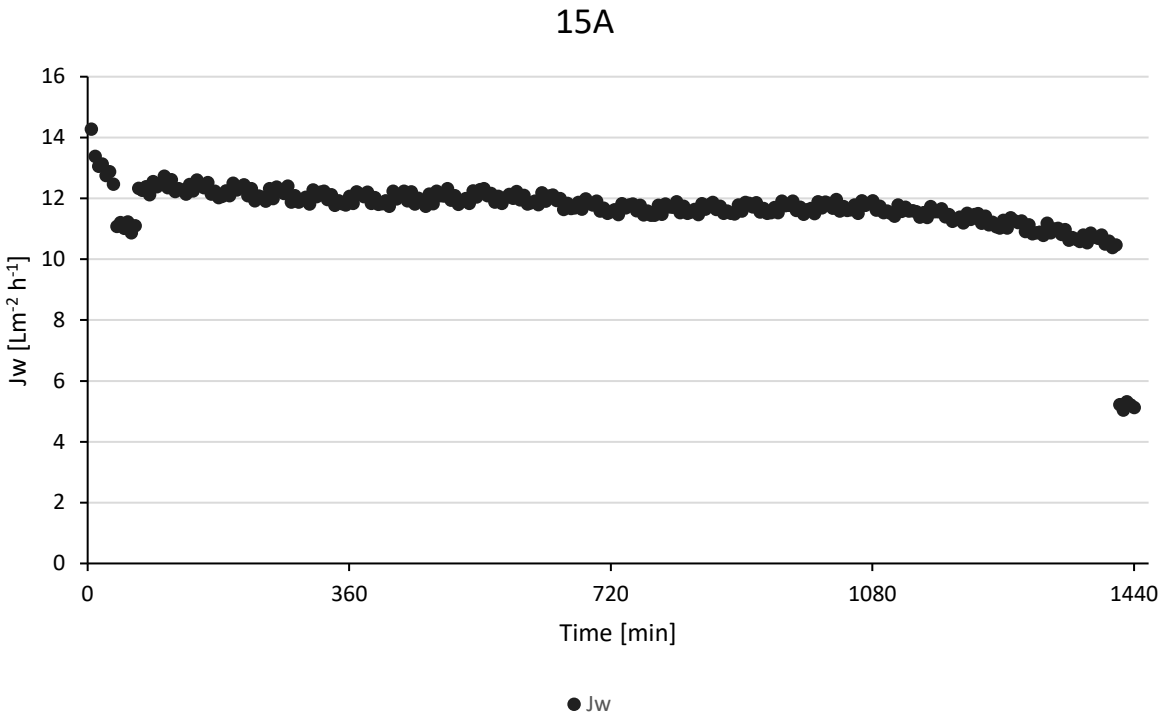

Figure S-33 Water flux (J_w) and solute back flux (J_s) during experiment 15 duplicate A.

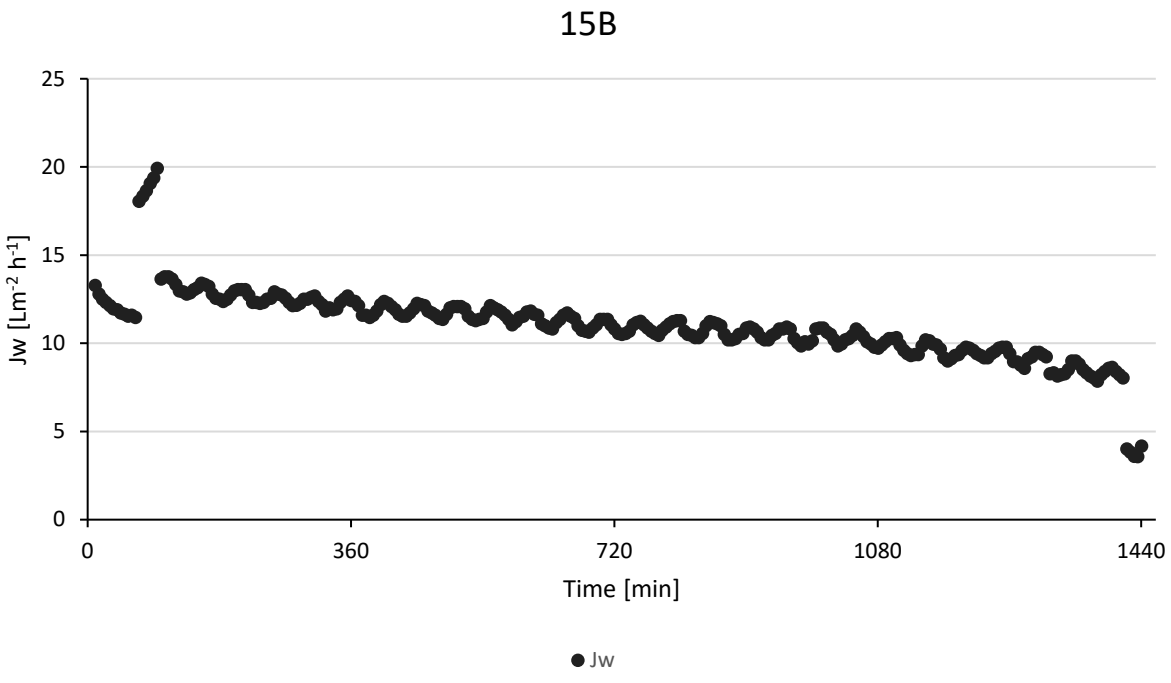

Figure S-34 Water flux (J_w) and solute back flux (J_s) during experiment 15 duplicate B.

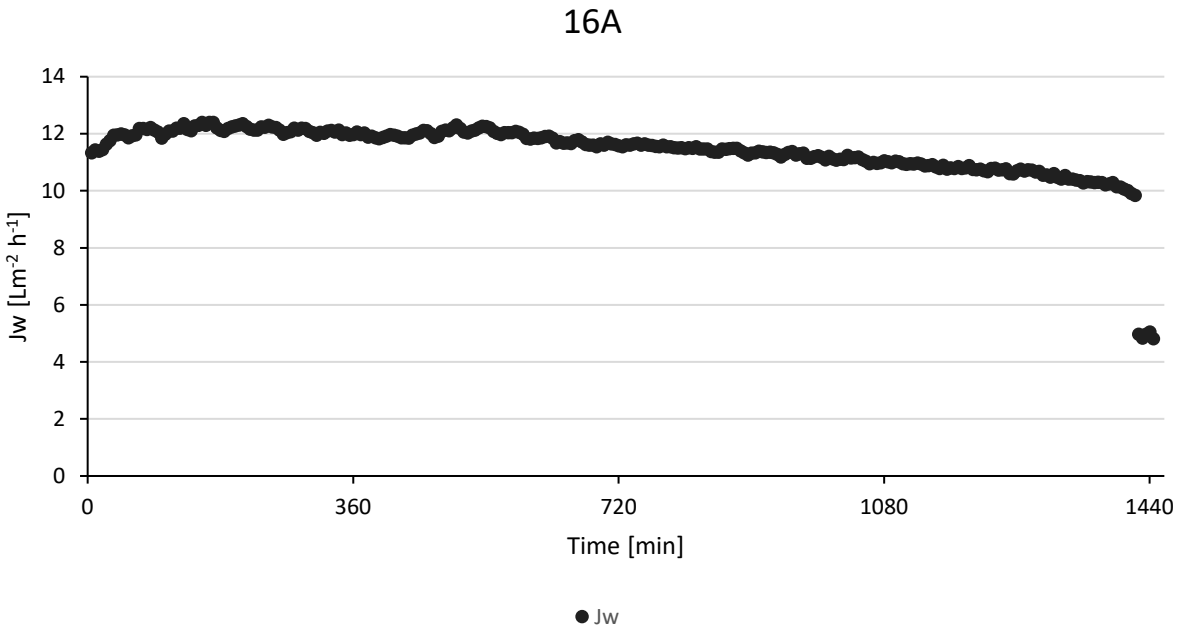

Figure S-35 Water flux (J_w) and solute back flux (J_s) during experiment 16 duplicate A.

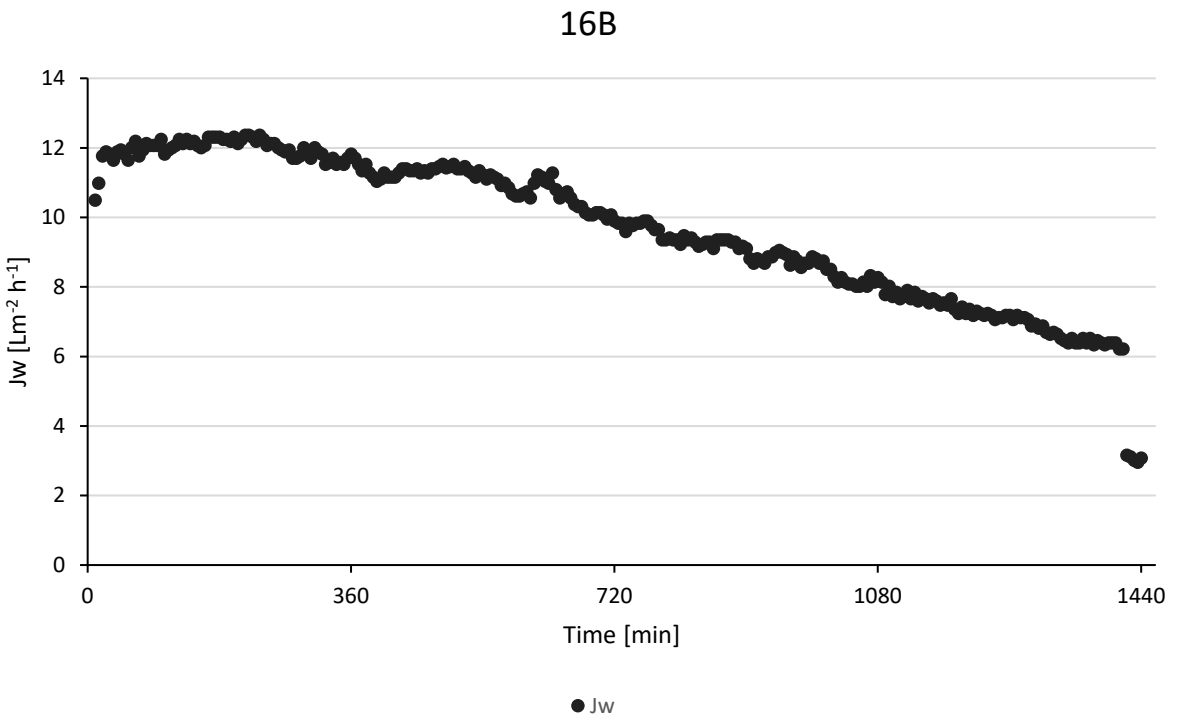

Figure S-36 Water flux (J_w) and solute back flux (J_s) during experiment 16 duplicate B.

5. Experimental data from methanotrophic batch assays and visual inspection of floc formation

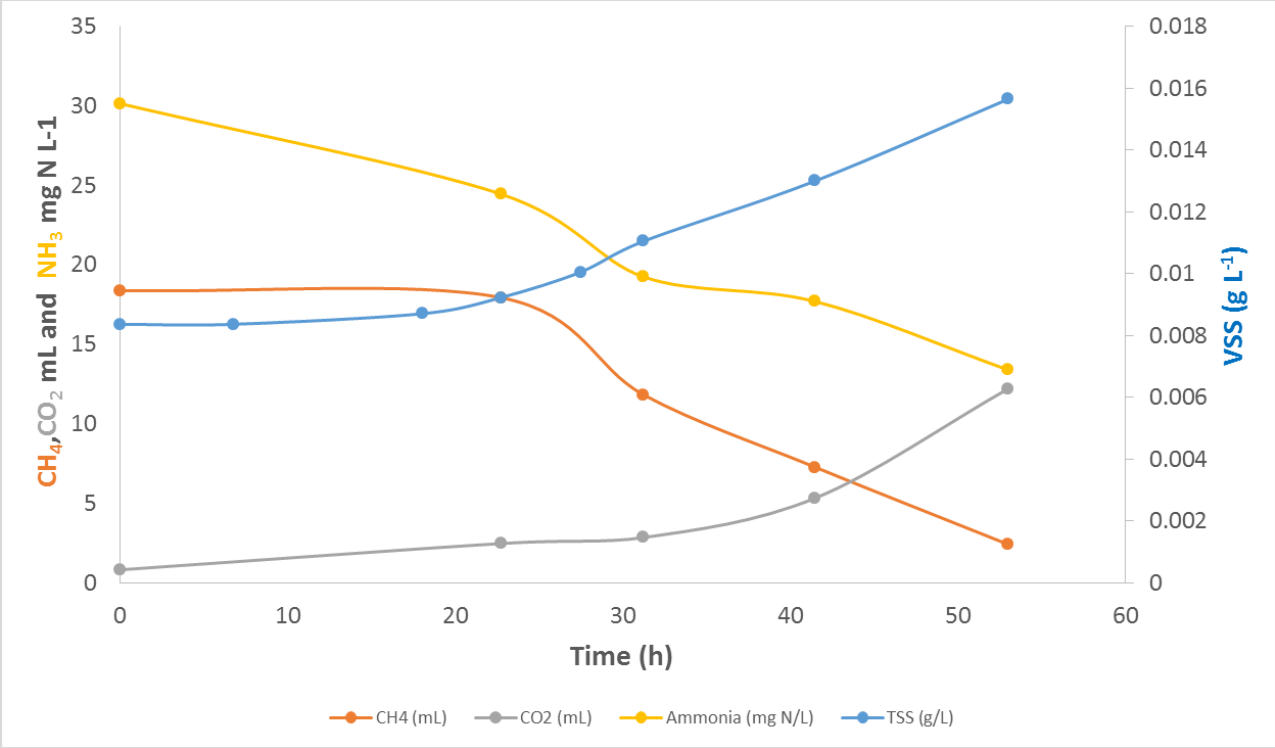

Figure S-37 Example of performance data for the batch assays – glycerol batch.

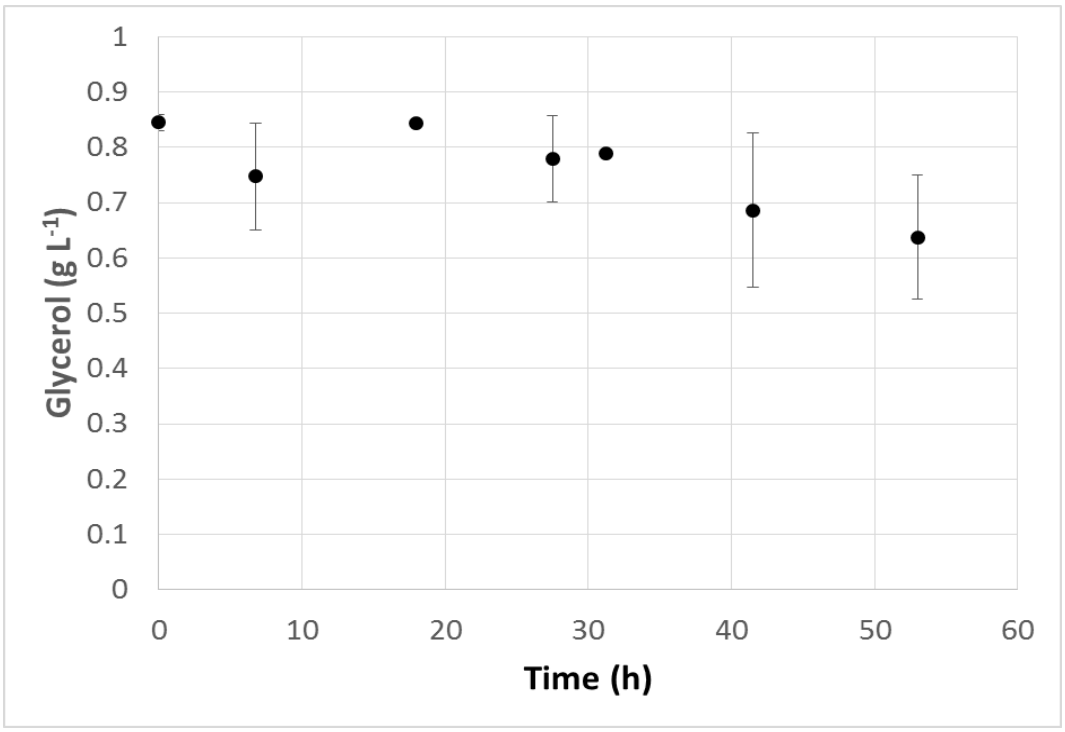

Figure S-38 Glycerol consumption during the batch cultivation.

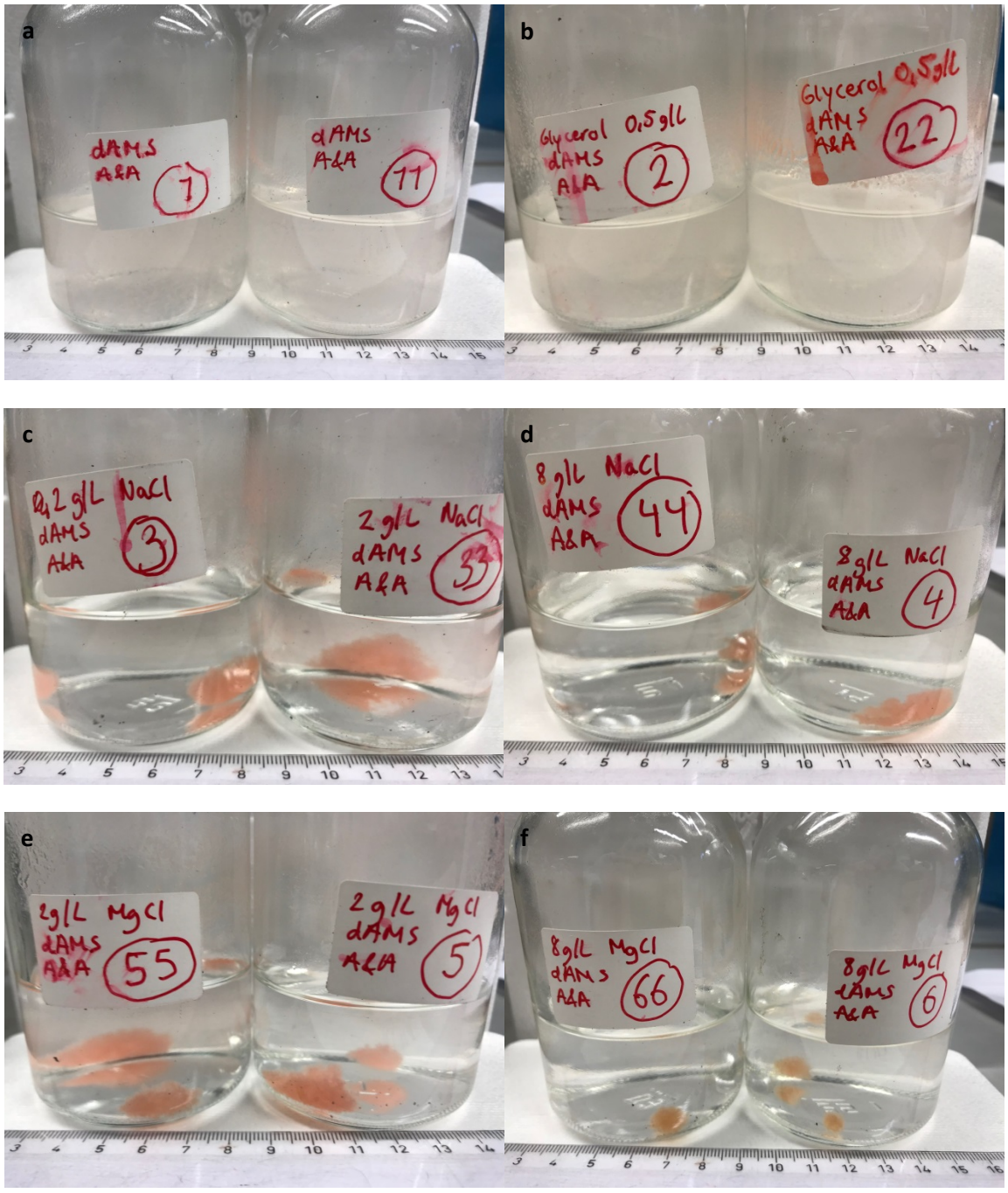

Figure S-39 Biomass flocculation during the batch cultivation at different draw solutes concentrations – a) default dAMS; b) 0.8 g L^{-1} glycerol; c) 2 g L^{-1} NaCl; d) 8 g L^{-1} NaCl; e)2 g L^{-1} $MgCl_2$; f) 8 g L^{-1} $MgCl_2$.